Delft University of Technology

Electrical Engineering, Mathematics and Computer Sciences

High Voltage Technology and Asset Management

Master of Science Thesis

Framework of Model-Based Health Optimization on the Electrical Power System

Ricardo dos Santos Grizonic, 4065344

Delft, The Netherlands

9 of April of 2013

"Millions saw the apple fall, but Newton asked why."

Bernard Baruch

Abstract

The advanced ageing of the electrical power network combined with the inevitable increase of renewable energy utilization and the constant increase of power consumption over the last decades call for a change in the current power network paradigm. Electrical world stakeholders have to embrace the situation and come up with methods of better utilizing the existing, but also new, network resources. The ongoing financial crisis also acted as an eye opener for new concepts and smart opportunities.

This project's approach is to create a modern and automated layer on top of the existing power network physical layer which makes use of several physical models to interpret the current and future expected health status of the network's components. With this automated layer, the network operator can configure the network to be a self-sustainable, or at least more independent, and a more insightful system. Real-time and projections of the network's health status can be used as power flow optimization factors.

Simulations based on real power flow data have shown that distributing thermal loading throughout neighbouring power components results in a more efficient resource utilization as it lowers the overall network accelerated ageing factor, while keeping the power flow characteristics within the legislated integrity limits.

It has been shown that, by applying this health prediction framework to the IEEE-14 bus network and allowing the layer to act in a decentralized fashion independently of the network operator, the overall network lifetime utilization can be reduced by 80% by rerouteing only 13% of the overall power flow. This rerouteing of power flow does not compromise the load requirements, nor does it require more power components than the ones present in the IEEE-14 bus network configuration.

Although it is difficult to implement this framework layer on top of the electrical power network, due to its well-known structural inertia, it has been shown that this system can effectively be deployed in different steps in time. Furthermore, the level of trust the network operator has in the system can also be incrementally upgraded, as this layer can be used at first simply as a more insightful source of data and only when desired it can be used as a more active factor in the electrical power network management.

Keywords: model-based optimization, power transformer, oil-paper insulation, insulation ageing, asset management, smart grid, renewable energy integration, high frequency transients decision making, IEEE14, MATPOWER, Matlab, High Voltage, tangent delta, Tettex 2840, agent, electrical power network, predictive health model, thermal loading.

Acknowledgements

I see this document as the culmination of long itinerary. Although only my name shows up in the cover page, many individuals have actively participated in the process.

First of all, I would like to express my appreciation to my supervisor Dhiradj Djairam for guiding me throughout the development of this project. I would also like to offer my special thanks to Professor Johan Smit and Professor Marian Popov for joining my thesis committee.

Advice given by Ing. Paul van Nes and Wim Termorshuizen has been a great help during the laboratory research phase of the project. For that, thank you.

My thanks are extended to the staff of Calendar42 for all the support throughout this period. I would like to leave a special appreciation note towards Michel Boerrigter and Jasper Hartong who were extraordinarily understanding and allowed my student and worker lives to harmoniously coexist.

I am particularly grateful for the opportunity created by the Portuguese foundation Maria Inês de Menezes Vaz de Sampaio. Mere words are not enough to describe my gratitude towards you.

I also take this opportunity to express a deep sense of gratitude to my former IST/Erasmus colleagues with whom I had many long, yet extremely interesting, discussions about anything that would pop up in minds. For them, Henrique, Falcão, Carreira, Sílvio, Meireles, and Batista, a big thanks.

I would also like to leave a big recognition *bitaite* to the 27's guys that have always been there for me. Whatever, wherever, whenever. Thanks.

The unconditional support provided by my Mother is a large part of the results. Although not next door, you are always here, always caring, always loving. For all that, and much more, Thank You. To my Father, a big Thanks. You are a big pillar of the foundations. I owe my sister, Rita, for being a constant support and role-model throughout my life. Thank you.

Last, but definitely not least, a heartfelt thanks goes to my girlfriend Sara for all her patience, support, understanding, and love, during all the good and bad moments of this process. All the lost trips, concerts, shows, parties, walks, dinners, will soon be recovered! :)

Contents

List of Figures

List of Tables

Chapter 1

Introduction

The future demands a highly drastic change in the current energy world. The ongoing Energy Roadmap 2050 [1] released by the European Union, states that although the electrical energy consumption will increase by 41%, Europe has to achieve a reduction of greenhouse gases (GHG) emissions by 80% in comparison to 1990. Given these strict and ambitious objectives, it is clear that several aspects must be changed in our current view regarding the needs of our energy system.

According to the Roadmap 2050 [1], several steps need to be taken to accomplish this decarbonization, namely:

- energy efficiency increase of 2% per year;
- increase the electricity stake in the energy domain - around 65%;
- substantial spread of the usage of Renewable Energy Sources (RES) - achieving at least 55% of total in 2050;
- centralised and decentralized systems increasingly interact - mainly due to the increase of RES.

A vast part of the electrical power system in place today has been built 30 to 40 years ago. Not only is most of the power system's components reaching the end of its lifetime, but also, at the time such systems were planned and designed, the existing political regulations, technical conditions, and electricity usage were not comparable to the ones that society, energy parties and environmental issues impose today. There are several types of new challenges to the electrical power system. A good example is the demand for the introduction of RES in the electrical production backbone. Two practical consequent outcomes that change the existing design and planning paradigms are the need to encompass intermittent power sources[1] and the inevitable

[1] power sources that one can not fully trust for production, as they might shut down at any moment throughout the production period - wind and solar energy.

introduction of high frequency harmonics in the power flow. These high frequency harmonics are introduced in the power flow by the transients generated in the power electronics systems necessary to enable the usage of most RES.

Moreover, an important factor that has occurred throughout the last decades is the continuous increase in power demand. Given the durable condition of most power network components (several high voltage components have a lifetime expectation of 40 to 50 years), only over the last decade, the urge of asset monitoring and maintenance has bacome relevant [22]. Furthermore, as components such as power transformers can withstand temporary overloads without immediate visible detrimental results, network operators might sometimes ignore the requirement to increase the power network's transmission capacity.

As shown in [3] and [4] both heat and high frequency harmonics can decrease the estimated lifetime of a power network component due to insulation degradation.

As a result of the advanced age of the current power network a major set of infrastructural investments needs to take place over the next decade. The electrical system that will be in place around 2050 has to be planned and built over the upcoming ten years. This planning should encompass the fact that, although the theoretical lifetime of a component such as a transformer (>25MVA) is around 40 years, recent studies [2] have shown that the lifetime of a transformer can be considered unpredictable. Average lifetimes of 18 years have been reported by these studies and they relate this average value to insulation failures, the most common failure case in the transformer world. With an increase of the number and complexity of the existing challenges, planning, monitoring, and maintenance will take key roles in this expected power network restructuring.

1.1 Ongoing changes in the Electrical Power World

1.1.1 Sustainable Energy

The concept of Sustainable Energy was officially originated by the Brundtland Commission from 1983 and the word "sustainability" was only adopted around 42 years ago in the Cocoyoc Declaration. Nevertheless, according to [6], sustainability is a concept that can be traced back 4000 years. Furthermore, by the year 1257, in London, the pollution degree was so dramatic that within 50 years the death penalty was introduced for anyone burning coal. This measure lasted for 100 years.

Sustainable Energy is energy that provides for the energy needs of today without compromising the energy needs of future generations. Renewable energy sources are frequently misleadingly regarded as a synonym of Sustainable Energy. Renewable energy sources are one major part of the process, but certainly not the only one. A lot more factors are commonly listed as steps to attain energy sustainability, such as:

- reduction of energy consumption;
- sharing things we do not use all the time, such as vehicles;
- diversification of energy sources, both in type and location;
- utilization of efficient energy production and consumption technologies;
- production distribution, by means of microgeneration at the consumption point;
- storage, to effectively oppose the issue of RES intermittency;

1.1.2 Renewable Energy Sources

Renewable energy flows involve natural phenomena such as sunlight, wind, tides, plant growth, and geothermal heat, as the International Energy Agency explains[16]:

> *Renewable energy is derived from natural processes that are replenished constantly. In its various forms, it derives directly from the sun, or from heat generated deep within the earth. Included in the definition is electricity and heat generated from solar, wind, ocean, hydropower, biomass, geothermal resources, and biofuels and hydrogen derived from renewable resources.*

Throughout the history of electric energy production the most utilized energy sources were not renewable ones, in the human time scale. Nowadays, there is a thrive to move the most we can towards renewable energy sources, such as wind, water, sun, etc. These energy sources result in a much cleaner electricity production, as there is, mostly, no carbon oxides (and other GHG) released to the atmosphere. Moreover, renewable energy sources still present quite some issues to be fought, namely the high production costs and its production uncertainty. RES are, in general, intermittent sources. For example, the wind does not blow throughout the whole day, and therefore the utilities can not fully depend on it to serve power to their costumers.

This source intermittency remains a major issue to be solved. Although there are several possible solutions, they all involve a large network restructuring or at least a great investment in new paradigms. Within the possible solutions, the most discussed ones are: energy storage and power source diversity. If the source is not available at all times, one can take advantage of its available times to, for example, pump up hydroelectric systems and therefore transform the electricity provided from the renewable sources into gravitational potential energy. This gravitational potential energy can, of course, be used at any moment the renewable sources cease to be a reliable solution for the base load.

As an alternative or, ideally, a supplement to the solution, we can also broaden the diversity of RES and, in that way, reduce the intermittency likelihood.

1.1.3 Distributed generation

Distributed power generators are usually small, modular electricity generators sited close to the customer load. They offers advantages that typical large-scale, capital-intensive, central-station power plants and distribution systems cannot provide. By using smaller, more fuel-flexible systems near the energy consumer, distributed generation avoids transmission and distribution power losses, and provides a wider choice of energy systems to the utility customer. This combined with the fact that distributed power generation has been shown to offer reliable, cost-effective, high-quality power during peak demand periods and to be a viable alternative to central station generated power.

Also, many distributed power systems produce so little noise and emissions that they can be located near the buildings where the power is needed, greatly simplifying the problems of conventional distribution infrastructure development. Distributed power generation technologies can use a variety of fuels, including natural gas, diesel, biomass-derived fuels, fuel oil, propane, and hydrogen. Fuel sources are also often based on renewable energy sources such as photovoltaic, wind and micro hydro, thereby further enhancing the positive environmental impact of a distributed power generation system. With renewed interest in the 1997 Kyoto Protocol, renewable energy and distributed power generation will become increasingly important as counties attempt to reach their emission requirements.

Distributed generation technologies yield power in capacities that range from a fraction of $1kW$ to about $100MW$. Utility-scale generation units generate power in capacities that often reach beyond $1GW$.

1.1.4 Smart Grid

There is a great deal of variation to what exactly should be included under the umbrella of a smart grid – it is not only the concept of developing smart meters or home automation, rather there is much more to consider. For instance, according to [17, 18, 19], the smart grid refers to a way of operating the power system using communications, power electronics, and storage technologies to balance production and consumption at all levels. Smart grid may be defined by its capabilities and operational characteristics rather than by the use of any particular technology. Broadly speaking, three major components of the smart grids are distributed intelligence, communication technologies, and automated control systems.

1.2 Thesis Motivation

The drivers for change in energy infrastructure are both external (low-carbon future) and internal (ageing infrastructure). The existing electric grid is not performing at the same level as it was decades ago. Energy losses in the transmission and distribution systems have nearly doubled from 1970 to 2001. Generally speaking, up to 8% of the electric energy leaving a power plant is lost in the transmission and distribution networks in most of the advanced power systems [21]. Energy efficiency has now became a key factor in the energy world. There are considerable security risks in the design of the grid with centralized generation plants serving remotely located loads over long transmission networks. Large scale development of RES has received special attention because they are environmentally friendly. However, integration of RES into the existing power network may bring many technical challenges associated with power quality, reliability, and security. The consumers are interested in getting more information and better control over their energy usage, e.g. smart metering can allow utility customers to take advantage of time-of-use pricing that was formerly available only to large commercial/industrial users. It has become apparent that the grid we know today is insufficient to serve in future and we need an innovative grid to meet the requirements and challenges of the future energy infrastructure.

Given the topics previously detailed, the future electrical infrastructure will demand many changes in its planning, monitoring, and management. The available lifetime of operating network components is a key factor present in all the aforementioned expected changes. This key factor can be assessed by means of online component monitoring, based on previously created models. Overall network lifetime knowledge allows the network operator to better plan and manage the overall network integrity.

As further explained in chapter 2, the lifetime of a component is highly variable with its utilisation rate. For example, with a very small increase of load on a power transformer, so that its temperature rises above the rated temperature, one can achieve highly accelerated ageing rates of the most fragile parts of the transformer, its windings insulation. Most power transformers currently in operation are equipped with oil-impregnated paper insulation [13]. Nowadays, the method the network operator uses to dispatch power in the most financially efficient way is to calculate the best scenario between generation and transmission costs, given that the transmission costs are mainly power losses in the line. The overall asset utilisation would definitely be more efficiently performed with the inclusion of the component's ageing factor as a key factor in the best power flow calculation, such as the generation costs and the transmission losses already are.

1.2.1 Research Objectives

The goal of this thesis is to study the possibility of creating a framework of power components' lifetime estimation that could be applied to any electrical network component, by varying the used models. The technical viability of such framework is tested through computer simulations.

Given these objectives, the following research questions are proposed:

- How does the power components' insulation react to temperature and high frequency transients?

- Which models can be used to assess a power component's ageing factor in operation?
- What kind of framework can be applied to all kinds of network components, in order to translate state variables into valuable actions for the system?
- Can this framework be applied on-site by the usage of an automated system (agent)?
- How can we efficiently make use of the framework's output to improve the performance of the network operator control centre?
- Is it possible to decentralise the control system throughout the network to capacitate the network with a dynamic self-controlling system?
- Can we make use of the framework, not only to know the current network status, but also to accurately predict it within a time interval?

1.2.2 Thesis approach

The first step is to assess the existing material over the proposed research questions. The objective regarding the optimization framework is to be usable in any electrical grid component. Nevertheless, in order to effectively test the system, a power transformer will be used as the test component. Important factors as what is a power transformer or how it behaves in operation will be regarded. A careful look will also be taken at what are the critical points of a power transformer's integrity and how one can use that information to extrapolate useful health status data.

After that, in order to better understand the existing power transformer's insulation models, some of the experiments reported in previous documents will be reproduced in a high voltage laboratory. This step is taken not only to better understand the insulation of the transformer, but also to attempt to improve some of the researched models. For example, the effect of high frequency transients in oil-impregnated paper will be assessed in the laboratory, as the existing scientific material about it is rather limited.

The third step is to plan and design the aforementioned optimisation framework that will enable us to translate the state variables of a network component into meaningful health status indexes. An example will then be further detailed regarding the operation of a power transformer, by the usage of the previously studied lifetime assessment models.

To verify the usability of such a framework, computer simulations are executed with the inclusion of automated agents equipped with the optimisation framework in each power transformer of the electrical network, in order to, based on a regular power flow simulation, read the outputs of these agents. With these outputs, the centralised control unit will have a better understanding of the network situation, especially because the agents also provide the network operator with a prediction horizon of what would happen in the case the power flow remained the same throughout a certain period of time (prediction horizon).

Further studies are performed over certain variation of factors, such as the prediction horizon, the presence of high frequency harmonics, due to the existence of RES in the network, etc.

At last, a look will also be taken at the possibility of decentralising the control unit into on-site actuators that react to the outputs of the nearby agents.

1.3 Publications

The work reported in this document has been referenced by the following publications:

- Djairam, D.; Grizonic, R.; Zhuang, Q.; Smit, J.J., "Developing the physical layer of future power grids: Required for automated asset management and renewable energy integration," Condition Monitoring and Diagnosis (CMD), 2012 International Conference on , vol., no., pp.509,512, 23-27 Sept. 2012;
- "Extending life time of high voltage components using predictive health management" by D.Djairam, T.L. Koltunowicz, G. Bajracharya, R. Grizonic, J.J. Smit.

1.4 Thesis Contents

The project behind this document is structurally divided in two different sub-projects:

1. research and development of oil-impregnated paper insulation models;
2. development and implementation of a health prediction framework that uses the physical models to improve the resource utilization efficiency by network operators.

In chapter 2, one can find the theoretical foundations that support both the aforementioned topics. As the power transformer is the example asset used throughout the project, section 2.1 encompasses the basics of the power transformer's components and their most relevant characteristics. Furthermore, in section 2.2, a detailed analysis of a transformer's thermal loading is performed. The influence of a transformer's thermal loading in its oil-impregnated paper insulation lifetime in postulated in section 2.3. An analysis of previous work on the effect of temperature cycling and high frequency transients in the transformer's health status is performed in section 2.4. Finally, a detailed view over the several methods for electrical power rerouteing is prepared is section 2.5.

Chapter 3 reflects an attempt to reproduce and further research the material studied in section 2.4. Throughout the chapter, one can find the laboratory set-up (section 3.1) and the results obtained in this project (section 3.2).

A framework of model-based optimization is proposed in chapter 4, where all the specifications for the application of the framework on a single power component can be found. Simulations of its applicability on a single and isolated power component are also performed in section 4.2.

The introduction of framework implementing agents in the power network is posited throughout chapter 5. A centralized control perspective is thoroughly detailed in section 5.1, whereas in section 5.2 one can find the same implementation in a decentralized control perspective. This chapter also encompasses simulations of example power networks with real power flow data, in order to generate a practical overview of the several detailed problems and their solutions.

In chapter 6, all the project results are discussed, including the overall viability of the concept.

Finally, conclusions and future work recommendations are detailed in chapter 7.

Chapter 2

Theoretical Background

Understanding, measuring, and modelling power transformer's dynamics has been a hot research topic over the last years [24, 25, 26, 27, 28, 29, 30, 31, 32]. On one hand, this is the case due to the increasing importance of achieving an accurate estimation of the power network components health state, considering its highly advanced ageing[1]. On the other hand, more types of models had to be recently developed in response to the presence of a new set of harmful factors caused by the growth of utilization of power electronics and the consequent decrease of power quality.

In the initial part of this chapter, a set of basic power transformer concepts and the most frequent ageing processes that occur in the transformer's components are explained. Furthermore, some issues and solutions are detailed about what types of state variables can be interpreted through the usage of literature models with the objective performing a better usage of the existing power network assets.

Different parties recommend distinct models and diverse approaches to face these issues. Along the following chapter, several models of power transformer's behaviour will be analysed. It is important to stress the fact that the main purpose of this project is to create a framework that could be a type of *Plug and Play*[2] system for the various types of possible health state models. The given models in the current chapter will integrate the system's testing included in chapters 4 and 5.

At last, a brief look is also taken at the most used power flow rerouteing techniques, as it is a solution to unload network components that are operating at a higher temperature than they were built for.

[1] as noted in chapter 1

[2] meaning that extra models could be hooked up in the framework with very little work from the system manager

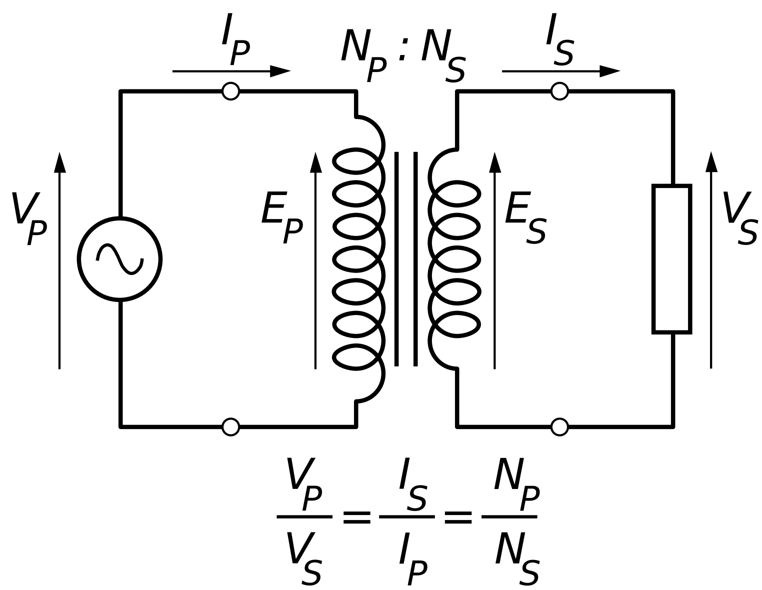

Figure 2.1.1 – Simplified Scheme of a Power Transformer.
Primary and secondary side voltages and currents are related through the transformer turns ratio. The higher the turns ratio (primary over secondary), the lower the voltage and higher the current on the secondary side of the transformer.

2.1 Transformers

A transformer is one of the most critical components of the electrical network that allows us to both efficiently transport electrical power at extremely high voltages and safely deliver electrical power to the consumers at the desired safe voltage level. A transformer is a type of power converter that can increase or decrease the line voltage (and therefore also the current) according to its turns ratio. Transformers connect two magnetically coupled circuits. When two circuits are magnetically coupled, the existence of a time varying current in the primary side inductively generates a varying current on the secondary side. The ratio between the current and voltage of the primary and secondary side are related through the transformer turns ratio, as shown in figure 2.1.1.

2.1.1 Core Steel

The purpose of a transformer core is to provide a low-reluctance path for the magnetic flux linking primary and secondary windings. In its core, the transformer experiences two types of power losses: hysteresis and eddy currents. Steel, the main material of the core is highly sensitive to magnetizing forces - good ferromagnetic material. As the magneto motive force (mmf) is alternating, for every cycle there will be extra work done inverting the magnetization of the core. For this reason, there will be a consumption of electrical energy which is known as the losses due to hysteresis. On one hand, these losses are proportional to the frequency and related to the characteristic of the material. On the other hand, the eddy current losses are dependent on the square of frequency but are also directly proportional to the square of the thickness of the material. Minimising hysteresis losses depends on the development of a material having a minimum area of hysteresis loop, while minimising eddy current loss is achieved by building up the core from a stack of thin laminations and increasing resistivity of the material in order to make it less easy for eddy currents to flow.

It is worthwhile to note that all the losses that occur in the core of the transformer produce heat that flows outwards through the insulation and cooling layers into the atmosphere. The more power lost in the core, the more heat travels through the insulation of the transformer.

Historically speaking, the first transformers manufactured in the 1880s had cores made from iron. However, in around the year 1900 it was recognised that the addition of small amounts of silicon or aluminium to the iron greatly reduced the magnetic losses [33].

2.1.2 Winding Conductors

Transformer windings are made almost exclusively of high-conductivity copper. Most of the copper used in transformer windings is in the form of rectangular-section wire or strip [33].

Current flowing through the windings causes resistive heating of the conductors. At higher frequencies, skin effect and proximity effect create additional winding resistance and losses. Resistive losses can be lessened by reducing the number of winding turns, by increasing the cross-sectional area of the turn conductor, or by a combination of both. Reducing the number of turns requires an increase in the core cross-section, which increases the iron weight and iron loss. As a result, load loss can be traded against iron loss and vice versa.

2.1.3 Insulation

Insulation is an extremely important part of the transformer. Internal insulation failures are invariably the most serious and costly of transformer problems. As power demand has been rising throughout the years, transformer rated voltages and MVA throughputs have continued to increase largely due to better use being made of the intrinsic value of the insulation. A vital aspect is the transformer life, and this is almost wholly dependent on the design and condition of the insulation. It must be adequate for a lifespan of 40 years or more and this probably explains the increasingly demanding testing regime of impulse testing, switching surges and partial discharge measurement.

2.1.3.1 Paper

Paper - pure cellulose - is among the cheapest and best electrical insulation material known. The important electrical properties of the paper as an insulation material are: high dielectric strength, dielectric constant in oil-filled transformers as close as possible a match to that of oil, low power factor (dielectric loss), and freedom from conducting particles.

2.1.3.2 Oil

Transformer oil is used both as an insulator and as coolant. For most transformers mineral oil is the most efficient medium for absorbing heat from the core and the windings and transmitting it, sometimes aided by forced circulation, to the naturally or artificially cooled outer surfaces of the transformer. The maximum allowed temperature within a power transformer is a characteristic influenced by the existence of paper in the insulation. If the transformer is to have an acceptable working life, then this temperature must be limited to somewhere around the $100^{\text{o}}C$ [33].

The oil is also required to make an important contribution to the efficiency of the solid insulation by penetrating into it and filling the spaces between layers of wound insulation. Impregnation also takes place with the mineral oil after the paper has been dried and degassed by exposure to vacuum.

Another critical note is that mineral oil is combustible - it has a fire point of $170^{\text{o}}C$ - and transformer fires do sometimes occur. It is usual, therefore, to locate these outdoors where a fire is more easily dealt with and consequentially the risks are fewer.

2.1.4 Tap Changer

A transformer tap is a connection point along a transformer winding that allows a certain number of turns to be selected. This means that a transformer with a variable turns ratio is produced, enabling voltage regulation of the output. The tap selection is made via a tap changer mechanism. In the case of large and important transformers, this procedure can be done on-load. On large power transformers taps of $\pm 10\%$ or more might be provided, selectable by means of on-load tap-changers [33].

2.1.5 Current Paradigm

The population of power transformers is growing old. Once regarded as power transformers giants, requiring no particular attention, they are becoming a source of concern to utilities as the incidence of outages and explosions increases [13]. This concern is extended by the transformers' high current value, their long outage times, the high cost of replacing them, and the serious consequences of system failure. To minimize the need for reinvestments and costly maintenance, and to plan rationally for the future, it is essential to understand and quantify the ageing kinetics and to learn how they may be controlled. In this context, the windings are the most vulnerable part of the transformer. The winding insulation system is subject to irreversible and significant ageing. Although failure rates are still low, one can foresee a future in which ageing of the celluloid insulation system has resulted in a reduced ability to withstand the mechanical stresses occurring during inrush currents and external short circuiting. The problem is accentuated by changes in operational conditions, including increases in humidity, increased loading, etc. Several significant experimental studies have established that temperature, moisture, and oxygen are major factors influencing the ageing of cellulose in transformers [13, 14, 15].

2.2 Dynamic Thermal Loading of Transformers

The thermal models used in this thesis are based on the IEEE C57.91's recommendations [4], but also take into account the changes in oil viscosity and loss variation referred in [7] as key factors. The transformer thermodynamics can be broadly described by the top-oil (θ_{oil}) and the hot-spot (θ_{hs}) temperatures.

$$\theta_{oil} = \theta_{amb} + \Delta\theta_{oil} \tag{2.2.1}$$

$$\theta_{hs} = \theta_{amb} + \Delta\theta_{oil} + \Delta\theta_{hs} = \theta_{oil} + \Delta\theta_{hs} \tag{2.2.2}$$

where θ_{amb} is the ambient temperature and Δ represents a positive variation of temperature. From equation 2.2.2, it is straightforward that, as the names indicate, the hot-spot temperature of a power transformer will always be higher than the top-oil temperature under operation.

Most of the equations in this section and throughout the remaining document consider electrical variables to be in per-unit (pu). In the power transmission field of electrical engineering, a per-unit system is the expression of system quantities as fractions of a defined base unit quantity. Calculations are simplified because quantities expressed as per-unit are the same regardless of the voltage level. Similar types of apparatus will have impedances, voltage drops and losses that are the same when expressed as a per-unit fraction of the equipment rating, even if the unit size varies widely. Conversion of per-unit quantities to volts, ohms, or amperes requires a knowledge of the base that the per-unit quantities were referenced to.

2.2.1 Top-Oil Temperature

The top-oil temperature can be both obtained by direct measurement or calculation. Direct measurement of this value is, most of the times, unavailable. Therefore, a model based on the ambient temperature, loading, and physical properties of the transformer has been proposed in

[7] to better represent the dynamics of a transformer's top-oil temperature:

$$\frac{1+RK^2}{1+R}\mu_{pu}\left(\theta_{oil}\right)^n \Delta\theta_{oil,rated} = \mu_{pu}\left(\theta_{oil}\right)^n \tau_{oil,rated}\dot{\theta}_{oil} + \frac{\left(\theta_{oil}-\theta_{amb}\right)^{n+1}}{\Delta\theta_{oil,rated}^{n}} \quad (2.2.3)$$

where K is the load factor in per-unit, R is the ratio of load loss at rated load to no-load loss on the tap position to be studied, $\Delta\theta_{oil,rated}$ is the top-oil temperature rise over the ambient temperature at rated load on the tap position to be studied in $°C$, $\mu_{pu}\left(\theta_{oil}\right)$ is the variable oil viscosity in per-unit, $\tau_{oil,rated}$ is the rated top-oil time constant, n is a constant that depends on the transformer's type of cooling.

The rated top-oil time constant ($\tau_{oil,rated}$), in minutes, can be calculated based on:

$$\tau_{oil,rated} = \frac{0.48 M_{fluid}\Delta\theta_{oil,rated}}{P}60 \quad (2.2.4)$$

- M_{fluid} is the mass of the oil in kg;
- P is the total loss at the rated load in W.

The change in viscosity of oil at the top-oil temperature ($\mu_{pu}\left(\theta_{oil}\right)$) is given by [8]:

$$\mu\left(\theta_{oil}\right) = 0.0013573\exp\left(\frac{2797.3}{\theta_{oil}+273}\right) \quad (2.2.5)$$

$$\mu_{pu}\left(\theta_{oil}\right) = \frac{\mu\left(\theta_{oil}\right)}{\mu\left(\theta_{oil,rated}\right)} = \frac{\exp\left(\frac{2797.3}{\theta_{oil}+273}\right)}{\exp\left(\frac{2797.3}{\theta_{oil,rated}+273}\right)} \quad (2.2.6)$$

With a quick look, one can extrapolate from equation 2.2.3 that the rate of increase of the top-oil temperature - its derivative - is proportional to the square of the load factor of the transformer. However, its derivative decreases with the increase of its difference to the ambient temperature, as the thermal conduction to the atmosphere increases.

2.2.2 Hot-Spot Temperature

The temperature of a power transformer winding is not uniform and, therefore, the real limiting factor taken as reference to the transformer's integrity evaluation is actually the hottest section of the winding called winding hot-spot. This hot-spot area is located somewhere towards the top of the transformer, and not accessible for direct measurement with conventional methods. As stated in equation equation 2.2.2, the hot-spot temperature can be estimated based on the dynamics of the top-oil temperature. The model that represents the hot-spot temperature behaviour, taking into account the variance of losses ($P_{cu,pu}\left(\theta_{hs}\right)$) with temperature [7], is the following:

$$K^2 P_{cu,pu}\left(\theta_{hs}\right)\mu_{pu}\left(\theta_{oil}\right)^n \Delta\theta_{hs,rated} = \mu_{pu}\left(\theta_{oil}\right)^n \tau_{wdg,rated}\dot{\theta}_{hs} + \frac{\left(\theta_{hs}-\theta_{oil}\right)^{n+1}}{\Delta\theta_{hs,rated}^n} \tag{2.2.7}$$

where $\Delta\theta_{hs,rated}$ is the rated hot-spot temperature rise over the top-oil temperature and $\tau_{wdg,rated}$ is the rated hot-spot temperature time constant.

The aforementioned variable power losses ($P_{cu,pu}\left(\theta_{hs}\right)$), can be calculated based on [7]:

$$P_{cu,pu}\left(\theta_{hs}\right) = P_{cu,dc,pu}\frac{235+\theta_{hs}}{235+\theta_{hs,rated}} + P_{cu,eddy,pu}\frac{235+\theta_{hs,rated}}{235+\theta_{hs}} \tag{2.2.8}$$

- $P_{cu,dc,pu}$ are the DC losses in pu;
- $P_{cu,eddy,pu}$ are the eddy currents losses in pu;
- $\theta_{hs,rated}$ is the rated hot-spot temperature in ^{o}C.

The hot-spot temperature, similarly to the top-oil temperature, has an increase rate - its derivative - proportional to the square of the load factor of the transformer. Its derivative also decreases with the increase in its difference to the top-oil temperature. This result is, again, intuitively explained by the rise of thermal conductivity.

2.2.3 Computational Optimization of the Temperature Equations

Equations 2.2.2 and 2.2.7 are differential equations and solving them can be a heavy computational problem, because complex numerical methods have to be applied in order to find the solutions. Regarding this fact and realizing that for this kind of estimations the system does not need highly precise values, these equations can be simplified by using the Euler method[3], transforming them into discrete functions.

- By discretizing $\dot{\theta}_{oil} = \frac{\theta_{oil}(k+1)-\theta_{oil}(k)}{h}$ and $\dot{\theta}_{hs} = \frac{\theta_{hs}(k+1)-\theta_{hs}(k)}{h}$ the following equations result for the top-oil and hot-spot models:

$$\theta_{oil}(k+1) = \theta_{oil}(k) + \frac{h(\frac{1+RK^2}{1+R}\mu_{pu}\left(\theta_{oil}\right)^n \Delta\theta_{oil,rated} - \frac{\left(\theta_{oil}-\theta_{amb}\right)^{n+1}}{\Delta\theta_{oil,rated}^n})}{\mu_{pu}\left(\theta_{oil}\right)^n \tau_{oil,rated}} \tag{2.2.9}$$

$$\theta_{hs}(k+1) = \theta_{hs}(k) + \frac{h(K^2 P_{cu,pu}\left(\theta_{hs}\right)\mu_{pu}\left(\theta_{oil}\right)^n \Delta\theta_{hs,rated} - \frac{\left(\theta_{hs}-\theta_{oil}\right)^{n+1}}{\Delta\theta_{hs,rated}^n})}{\mu_{pu}\left(\theta_{oil}\right)^n \tau_{wdg,rated}} \tag{2.2.10}$$

where h can be considered as the prediction step. Some notes about the choice of the prediction step can be found in section 4.2.2.5.

[3]the Euler method is a first-order numerical procedure for solving ordinary differential equations with a given initial value.

As expected, both equations still retain the square dependence with the load factor and a negative dependence to the difference of temperature to the ambient temperature (in the case of equation 2.2.9) and to the top-oil temperature (in the case of equation 2.2.10).

2.3 Insulation Ageing Factors

Temperature, moisture, oxygen, amongst others are recurring physical factors that can accelerate the loss rate of the transformer insulation lifetime. Recent technologies provide us with an efficient way of preserving the oil condition, in order to diminish, or even extinguish, the contribution of factors like moisture and oxygen in the acceleration of the insulation ageing. According to [4], by making use of the described technologies of oil preservation, one must give an enhanced importance to the oil temperature behaviour and its share in the insulation ageing.

The transformer's insulation Per Unit Life (PUL) relates to the hot-spot temperature by means of an adapted Arrhenius reaction rate theory equation. As suggested by [5], this behaviour modelling can be both applied to distribution and power transformers, due to the use of the same type of material in their insulation. The recommended PUL equation in the case of transformers with a rated temperature of $110^{\text{o}}C$ is:

$$PUL = 2.00 \times 10^{-18} \exp\left(\frac{15000}{\theta_{hs} + 273}\right) \tag{2.3.1}$$

Per Unit Life is the basis for the calculation of the ageing acceleration factor (F_{AA}) of a transformer's insulation for a given load and temperature. It can be observed from equation 2.3.1 that the per unit life of the transformer's insulation decreases with the increase of the hot-spot temperature. Regarding this fact, one can relate the rated PUL and the current PUL in order to obtain the ageing acceleration factor compared to the rated behaviour:

$$F_{AA} = \frac{PUL(\theta_{rated})}{PUL(\theta_{hs})} = \exp\left(\frac{15000}{\theta_{rated} + 273} - \frac{15000}{\theta_{hs} + 273}\right) \tag{2.3.2}$$

From equation 2.3.2 and figure 2.3.1, it can be concluded that while operating the transformer at its rated temperature ($\theta_{hs} = \theta_{rated}$) the ageing of the transformer's insulation will follow the estimation of the manufacturer's design (F_{AA}=1). If the hot-spot temperature of the transformer exceeds its rated temperature then (as expected) the ageing of the insulation will be accelerated ($F_{AA} > 1$) and the other way around for temperatures lower than the rated temperature.

Having access to this type of models and to a dataset from a time period of a transformer's operation creates the possibility of calculation of the loss of lifetime of a transformer throughout

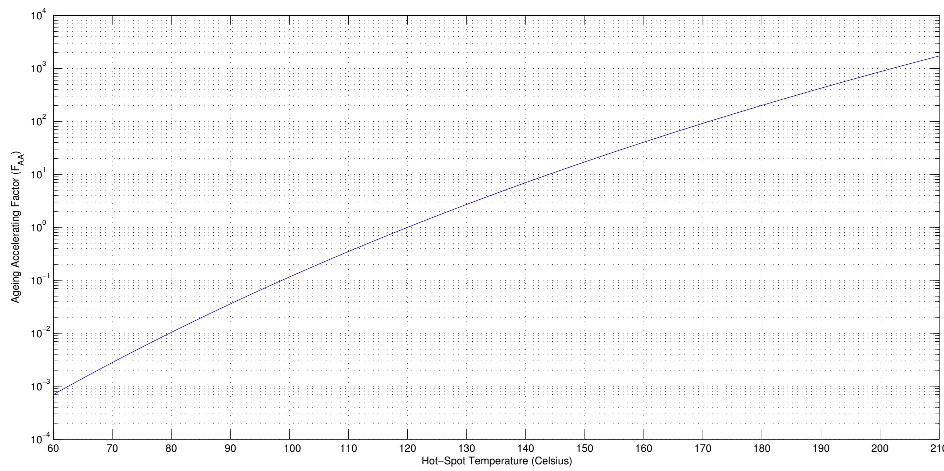

Figure 2.3.1 – F_{AA} exponential variation with the hot-spot temperature.
This plot shows the exponential variation of the acceleration ageing factor with the hot-spot temperature for a transformer with $\theta_{rated} = 120^{o}C$. Operating at the rated temperature, the acceleration ageing factor is 1, ($F_{AA}(120) = 1$).

that time frame, based on the estimation of the hot-spot temperature as given on section 2.2.2. The loss of lifetime (LLT) of a transformer's insulation during an operating period (T) where the average hot-spot temperature is $\theta_{hs,avg}$ can be obtained from:

$$LLT = F_{AA}T \tag{2.3.3}$$

The loss of lifetime obtained from the combination of equations 2.3.2 and 2.3.3 can be represented in the costs domain by using the following equation:

$$LC = \frac{LLT \times TC}{TLT} \tag{2.3.4}$$

where TLT is the Total Life Time estimated by the manufacturer, TC is the Total Cost of the device, and LC the cost of the lost insulation lifetime. This direct relation between lifetime loss and cost is presented in this document as a valid possibility due to the destructive influence that insulation failures have in power transformers. It is assumed that the failure of the insulation always causes a complete failure of the component.

2.4 Effect of Temperature Cycling and HF Transients on Oil-Impregnated Paper

In order to study the influence of on-load temperature cycling and transients on oil-impregnated paper insulation, in [9] tests are conducted on paper samples. The measurements are performed with samples that are electrically stressed while being heated to $40°C$, $60°C$, and $80°C$. The samples are electrically stressed by applying different waveforms. The AC waveform consists of a sinusoidal wave with an RMS value of $2.22kV$. A DC source simulates the transient behaviour of the grid[4] and this signal is be superimposed on the aforementioned AC waveform. The DC waveform consists of small spikes with a rate of rise of $1kV/\mu s$ and a repetition frequency between $1kHz$ and $10kHz$.

The author initially expected the dielectric properties of the paper samples to improve with the increase of the temperature, due to the consequently decrease of moisture in the paper configuration, as it is absorbed by the hot oil. Note also that the $\tan\delta$ decreases with the decrease of moisture content in the sample. When the transients are added to the waveforms, the author expects them to increase the $\tan\delta$ as they incite more vibration in the cellulose paper and, therefore, more dielectric losses.

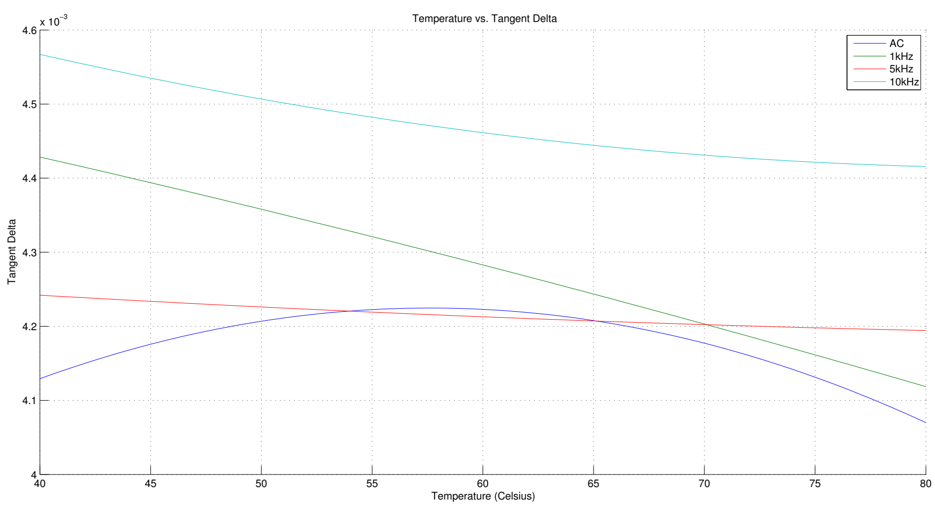

Figure 2.4.1 – $\tan\delta$ dependent on Frequency and Temperature
Four curves of the variation of the $\tan\delta$ with the temperature for a certain frequency are plotted. With the exception of the $5kHz$ curve, $\tan\delta$ increases with the frequency. If the AC only curve is not regarded, then $\tan\delta$ decreases with the increase of temperature.

[4]the intent is to simulate the transients produced by the power electronics intrinsically attached to the RES concept, as previously mentioned

From the summary of figure 2.4.1, it is clear that higher leakage losses in the insulation occur in the samples that were subject to transients of higher frequency. It is also noticeable that, contrary to the author's hypotheses, the $5kHz$ curve, for lower temperatures, is situated below the $1kHz$ curve. The proposed hypotheses remain valid for higher temperatures.

2.5 Power Flow Control

The following criteria govern the operation of an electric power system:

- Safety
- Quality
- Reliability
- Economy

The first criterion is the most important consideration and aims to ensure the safety of personnel, environment, and property in every aspect of system operations. Quality is defined in terms of variables, such as frequency and voltage, that must conform to certain standards to accommodate the requirements for proper operation of all loads connected to the system. Reliability of supply does not have to mean a constant supply of power, but it means that any break in the supply of power is one that is agreed to and tolerated by both supplier and consumer of electric power. Minimizing the generation cost and losses motivates the economy criterion while mitigating the adverse impact of power system operation on the environment.

As discussed in section 2.3, the lost lifetime of an asset can be directly translated into a financial cost. As a result, one of this project's proposal is to also include these lifetime losses in the aforementioned economy point. By doing so, the power flow calculation will not only regard the generation costs (fuel price, availability, etc.) and the transmission ohmic losses, but also the cost of the equipment usage in terms of its available lifetime. If we consider this as a critical factor in power flow transmission, then it is important to discuss how to efficiently perform power flow rerouteing, as the lifetime calculations can quickly change the optimal power flow paradigm. Consequently, it is important that the electrical network, and its operator, can promptly react to the system's decision. Along the next chapters more will be discussed about how the calculations are performed, how the data is transmitted, etc.

The power system operator has the following means to control system power flows:

- Prime mover and excitation control of generators;
- Switching of shunt capacitor banks, shunt reactors, and static var systems;
- Control of tap-changing and regulating transformers;
- FACTS based technology.

Tap changing and voltage magnitude regulating transformers are used to control bus voltages as well as reactive power flows on lines to which they are connected. In a similar manner, phase angle regulating transformers are used to control bus angles as well as real power flows on lines to which they are connected. Both tap changing and regulating transformers are modelled by a transformer with an off-nominal turns ratio. From the power flow point of view, a change in tap setting or voltage regulation corresponds to a change in tap ratio.

FACTS is an acronym for Flexible AC Transmission Systems. They use power electronic controlled devices to control power flows in a transmission network so as to increase power transfer capability and enhance controllability. The concept of flexibility of electric power transmission involves the ability to accommodate changes in the electric transmission system or operating conditions while maintaining sufficient steady state and transient margins.

Chapter 3

Temperature Cycling and HF Transients

In this chapter, a verification of the results in [9] is conducted. In order to facilitate the communication, throughout this chapter, the author's work will be called "Verification Results" and the previous work reported in [9] will be called "Original Results".

Throughout the research on the effect of temperature cycling and transients presented in the Original Results and the Verification Results, the main objective is to model the influence of these types of factors in the insulation of transformers, namely by studying the variation of the insulation's $\tan\delta$ with a large set of different detrimental factors. The Original Results are briefly described in section 2.4 and the Verification Results are described in a more detailed overview in section 3.2. Both researches took place in the same laboratory with, in theory, the exact same conditions detailed in section 3.1. Both outcomes are discussed in section 3.3.

The main target of the developed work by the author, while generating the Verification Results, is not only to verify the existing scientific work, but also to acquire a thorough insight over the behaviour characteristics of oil-impregnated paper insulation.

This chapter starts with an brief explanation of the laboratory set-up in section 3.1, followed by the experiments and results in section 3.2. Finally a comparison between both the Original Results and the Verification Results is performed in section 3.3, wrapped up by a summary section (3.4).

3.1 Laboratory Set-up and Procedure

In order to study the influence of temperature cycling and transients in the oil-impregnated paper insulation of power components, tests have been performed on single layers of oil-impregnated paper with a thickness of $60\mu m$. This paper, although previously oil-impregnated by the manufacturer, was also subjected to an impregnation reinforcement right before the initiation of the tests. This impregnation reinforcement consists on a period of $48h$ in a vacuum oven immersed in a tin filled with oil, at $100^{o}C$. Shell Diala B is the type of mineral oil used throughout these experiments.

The first test step, after the impregnation reinforcement, is to stress the sample at a certain voltage, temperature, and also with the occurrence of superimposed high frequency transients. The test set-up used for this purpose can be found in figures 3.1.1 and 3.1.2.

The paper samples are subjected to a large set of temperature and signal variations. The temperature test varies amongst these values: $\pm 20^{o}C$ (ambient temperature), $40^{o}C$, $60^{o}C$, and $80^{o}C$. The electrical stress also varies between tests, within the following set of values: AC only or AC superimposed with DC peaks simulating high frequency transients between $1kHz$ and $10kHz$. These thermal and electrical stresses last for 22 hours and one example of such a signal can be seen in figure 3.1.3, where the DC peaks occur with a frequency of $10kHz$ and the AC component has the frequency of the European power network ($50Hz$).

After these electrical and thermal stresses, a comprehensive study of the sample's $\tan\delta$ takes place. The $\tan\delta$ measurements were performed with a Tettex 2840 [10] device (figure 3.1.4) that has a Schering Bridge as its basic constitution. It is a device with a very high sensitivity, $\pm 5\% + 10^{-5}$, achieving very precise results in the measurement of the oil-impregnated paper insulation's $\tan\delta$ (average of 40×10^{-4}). In this device, the sample is placed between two electrodes that stress the sample with a voltage from around $50V$ up to $600V$. By measuring the leakage current that slips through the sample, a $\tan\delta$ value is quantified, and therefore the lifetime loss of the sample can be estimated.

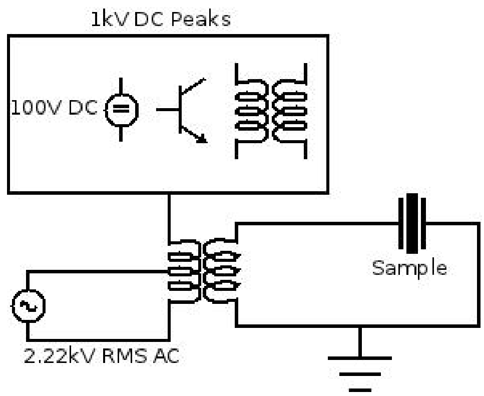

Figure 3.1.1 – Test Set-up of the Sample Stress Site
On the bottom left there is an AC voltage source that produces a $2.22kV$ RMS power signal which is superimposed by the high frequency spikes produced by the topmost box. These signals are transmitted by a transformer into the sample site on the right. One side of the sample is connected to a high voltage electrode and the other is earthed.

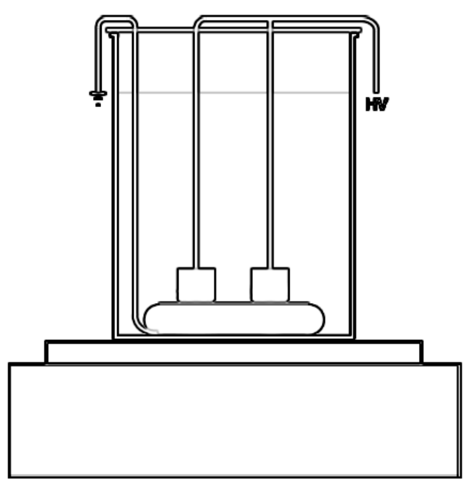

Figure 3.1.2 – Sample Site - Beaker with mineral oil is placed on top of a hot plate.
The oil-impregnated paper sample is placed between two small high voltage electrodes and a bigger ground electrode. The temperature of the hot plate is varied from $40^{o}C$ to $60^{o}C$, and up to $80^{o}C$.

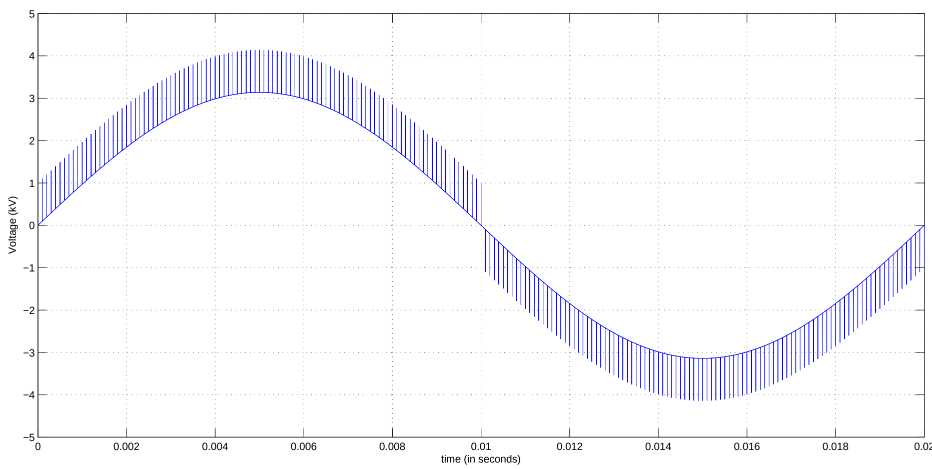

Figure 3.1.3 – Example High Voltage Stress Signal
This example signal is a superposition of a $2.22kV$ RMS AC wave with a high frequency spike signal that occurs at $10kHz$. The spikes have a magnitude of $1kV$ while the AC signal is on the positive cycle and $-1kV$ during the other cycle.

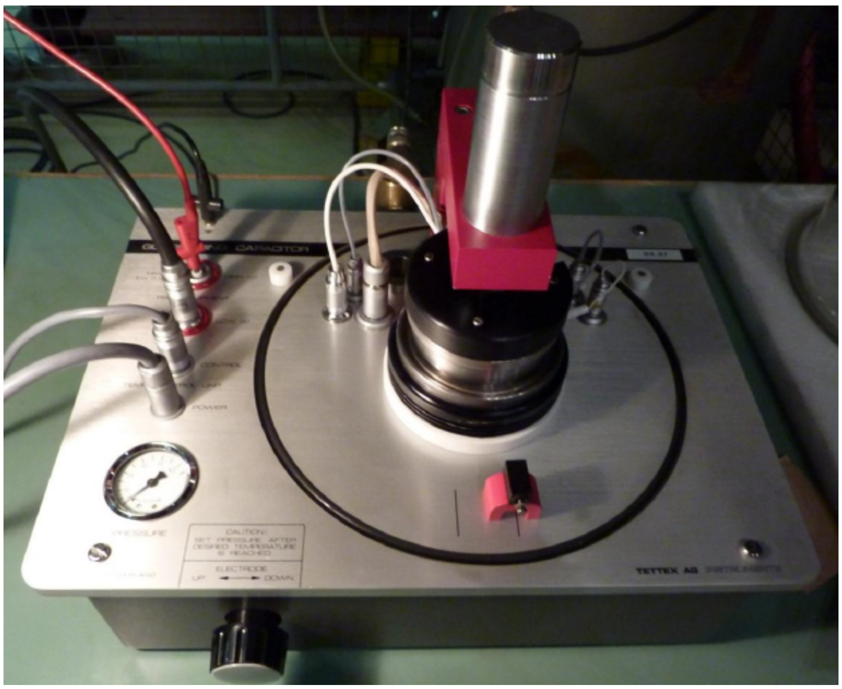

Figure 3.1.4 – Sample Test Site
This device is used to measure the leakage current of the paper samples. The sample is placed between two electrodes: the top one with a variable voltage ($50V$ to $600V$) and the bottom one is grounded. The outputted signal is then sent to a Schering-bridge-like device - Tettex 2840 - that interprets the leakage current and formulates a corresponding $\tan\delta$ for the sample.

3.2 Experiments and Results

With the initial objective of finding out why the outlier of figure 2.4.1 is present, this project was also based on some thorough laboratory work. All the procedures and environmental factors from [9] were replicated. Starting from the type of oil-impregnated paper, down to the pressure applied to the sample by the electrodes of the $\tan\delta$ measurement device, everything was planned with the target of matching the Original Results. Tests have been performed with the following conditions:

- Non-stressed samples;
- Thermal stress of $40^{\underline{o}}C$ with
  - →Absence of electrical stress
  - →AC only stress
  - →AC+5kHz transient stress

The first step for every sample is to reinforce its oil impregnation by submitting the sample completely submersed in a Diala B oil bucket to $48h$ of demoisturization inside a vacuum oven. Then each sample is subjected to the aforementioned stressing conditions. After the stressing step, each sample is individually tested for traces of degradation by the measurement of 36 data points of three sets of measurements from $50V$ and $600V$ with steps of $50V$, as can be seen in figure 3.2.1. The first set of 12 points[1] can be seen as a conditioning step. A conditioning step is characterized by the clearance of small impurities and air bubbles from the paper sample[2]. The two measurement runs after the initial conditioning step result in lower $\tan\delta$ values than throughout the first measurement run, which is intuitively explained by the reduction of impurities due to the conditioning. It is important to mention that most of these impurities and moisture are inevitably introduced into the sample structure while the test operator transports the sample between the stress site and the measurement site, due to its exposure to external factors such as the air. The action of trapping the sample between the measurement electrodes can also introduce air bubbles between the sample and the electrodes, which will also increase the resulting $\tan\delta$ measurement results.

On all the performed measurements, the procedure is the same, allowing us to compare the test results as seen in the following set of tables, where the values of $\tan\delta$ are shown in three types of format: per sample, globally averaged, and averaged with exclusion of outliers.

[1] the first set of data points are always the ones that depict the topmost curve
[2] these type of factors are related to an increase of the $\tan\delta$ measurement results

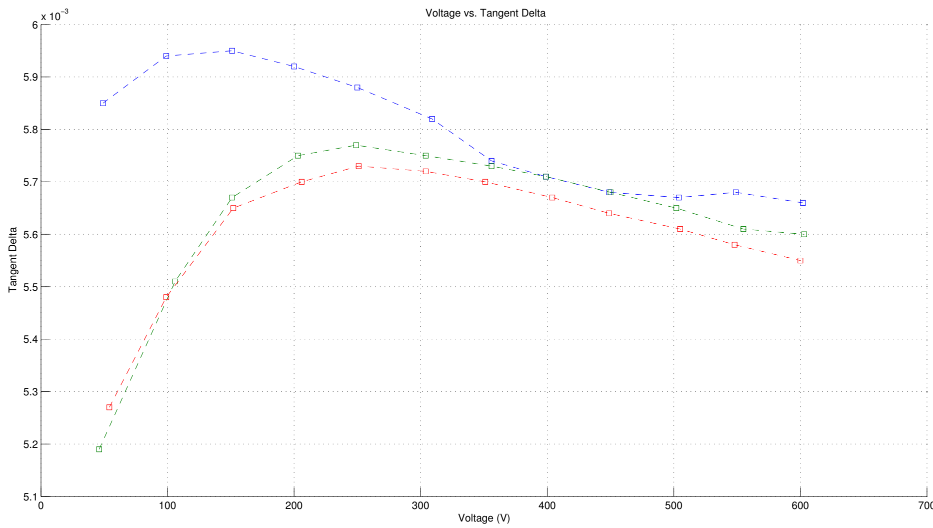

Figure 3.2.1 – $\tan\delta$ Measurement of a Stressed Sample
The $\tan\delta$ measurements are performed on a sample stressed with AC Only at 40^oC during $22h$. Three different curves can be plot from the three sets of measurements. The curve that has a higher $\tan\delta$ is the one that was performed first, as the sample still contains impurities that are then removed after some measurements (conditioning).

Table 3.1 – Set of Results of Non-Stressed Paper Samples, Stressed Samples with AC only at $40^{o}C$, and Stressed Samples with $AC + 5kHz$ transients at $40^{o}C$

Non-Stressed Samples		AC only - $40^{o}C$		$AC + 5kHz$ - $40^{o}C$	
Date	$\tan\delta_{AVG}$	Date	$\tan\delta_{AVG}$	Date	$\tan\delta_{AVG}$
2011-10-31	43.56×10^{-4}	2011-11-08	51.41×10^{-4}	2011-11-09	49.06×10^{-4}
2011-11-01	38.81×10^{-4}	2011-11-15	46.49×10^{-4}	2011-11-10	47.79×10^{-4}
2011-11-01	37.18×10^{-4}	2011-11-15	53.43×10^{-4}	2011-11-10	47.38×10^{-4}
2011-11-18	34.82×10^{-4}	2011-11-16	44.66×10^{-4}	2011-11-14	58.78×10^{-4}
2011-11-21	40.90×10^{-4}	2011-11-16	56.78×10^{-4}	2011-11-14	60.13×10^{-4}
2011-11-21	47.03×10^{-4}	2011-11-23	47.61×10^{-4}	2011-11-17	47.79×10^{-4}
		2011-11-23	44.25×10^{-4}	2011-11-17	43.36×10^{-4}
				2011-11-22	45.03×10^{-4}
				2011-11-22	42.94×10^{-4}
Average	40.38×10^{-4}	Average	49.23×10^{-4}	Average	49.14×10^{-4}
Average$\pm s$	40.11×10^{-4}	Average$\pm s$	48.72×10^{-4}	Average$\pm s$	46.19×10^{-4}

Identifying outliers can be a subjective task. In order to make this process a consistent procedure, the standard deviation concept will be used. For each result set, we calculate the standard deviation according to:

$$s = \sqrt{\frac{\sum(x_i - x)^2}{N - 1}} \tag{3.2.1}$$

and then all the values that confirm the following condition are filtered out:

$$\frac{(x_i - \bar{x})}{s} > 1 \tag{3.2.2}$$

By analysing table 3.1, it is clear that the average value of $\tan\delta$ for non-stressed samples is considerably lower than the values of the electrically stressed samples, both with AC only - $40^{o}C$ and $AC + 5kHz$ - $40^{o}C$. The difference between the samples stressed with AC only and the ones stressed with $AC + 5kHz$ transients is not so clear. Both results are very close[3] and, therefore, a distinction between the tests is difficult to posit. A discussion with further exposition can be found in section 3.3 on the facing page.

[3] 48.72×10^{-4} versus 46.19×10^{-4}

Table 3.2 – Comparison between both sets of experiments ($40^{o}C$)

	Original Results	Verification Results
Non-Stressed Sample	$\pm 40 \times 10^{-4}$	40.11×10^{-4}
AC Only ($40^{o}C$)	41.20×10^{-4}	48.72×10^{-4}
$AC + 1kHz$ ($40^{o}C$)	44.30×10^{-4}	NA
$AC + 5kHz$ ($40^{o}C$)	42.50×10^{-4}	46.19×10^{-4}
$AC + 10kHz$ ($40^{o}C$)	45.70×10^{-4}	NA

3.3 Original Results versus Verification Results

The samples' $\tan\delta$ decrease with the increase of the of the stress temperature. The only exception to this observation occurs in the AC only curve, where the $\tan\delta$ peak happens at $60^{o}C$. According to [9], this behaviour is explained by the decrease of moisture content of the paper, hence increasing its dielectric properties.

Regarding the behaviour of $\tan\delta$ with the superposition of transients to the stress signal shown in section 2.4, it can be said that, excluding the seemingly outlier curve of the $5kHz$ transients wave, the $\tan\delta$, and therefore the degradation of the insulation's lifetime, are higher with the increase of the transients frequency. The ageing of the samples is faster for higher transients frequency, because the cellulosic fibres vibrate along with the transient frequency, which highly degrades the paper constitution.

Analysing both sets of results, from sections 2.4 and 3.2 (in table 3.2), one can state that the starting point is a match: when measuring a new sample of paper (non-stressed) the results for the $\tan\delta$ seem to be a perfect match $\pm 40 \times 10^{-4}$ versus 40.11×10^{-4}. The divergence starts right after these first tests, when the tests include thermal and electrical stresses. It is fairly easy to see that there is a significant difference, not only regarding the absolute value of the results, but also their relative values.

Another important note to take is that, not only are the values presented in section 3.2 considerably higher than the ones from section 2.4, but there is also an inversion of the order of the values. The values obtained in section 3.2 would prove (if regarded as correct) that the inclusion of 5kHz transients in the electrical grid would actually improve the behaviour of the components insulation system.

There are many possible causes for this unexpected result, such as:

- different laboratory operator;
- the same material has been used (oil, paper, test setups, devices, etc), so perhaps something changed in the status of one or more of these elements;

Table 3.3 – Sample Failure Statistics

	$AC + 5kHz$	AC Only
Total Tests	26	8
Survived	9	7
Failures	17	1
% Failure	65.38	12.5

- only a very limited part of the samples survived to the stressing stage (table 3.3), and thus there is a limited set of data that could be considered as insufficient to postulate over the tendency of the studied material;

- the measured entities are characterized by quite precise values (10^{-4}), and therefore also prone to measurement errors;
- $\tan\delta$ measurements are, in general, very sensitive to perform. Extremely small quantities of impurities, variations in humidity, or air exposure can cause large variations in the obtained results.

Regardless of the divergence of results between both sections, the presence of electrical stress increases the leakage current in the layer. If only section 2.4 is taken into account, then it can also be said that transients are a factor that highly contributes to the increase of the $\tan\delta$ value.

The ageing acceleration can not be directly related to the increase of leakage current in the insulation layer. Nevertheless, if the leakage current increases, an increase of resistive losses and therefore an increase in temperature, can be anticipated. Although [4] suggests their existence, these leakage currents do not contribute to the temperature model posited in the document.

According to [11], an increase of $\tan\delta$ over time can be considered as a sign of deterioration of the insulation condition. Lifetime of the insulation layers is expected to be lower as the $\tan\delta$ increases. The exact value of $\tan\delta$ for which the insulation fails or how this lifetime degradation develops is still an unknown.

In [9], a new concept called "transient mix" is introduced, that emerges from the difficulty of individually classifying the transients influence in the $\tan\delta$ of a sample for each temperature. Regarding this fact, and observing table 3.4, a simple average of the transients influence is calculated:

$$\frac{\Delta\tan\delta_{40^{o}\mathrm{C}} + \Delta\tan\delta_{60^{o}\mathrm{C}} + \Delta\tan\delta_{80^{o}\mathrm{C}}}{3} = \frac{9.88 + 3.35 + 6.00}{3} = 6.4\% \tag{3.3.1}$$

This "transient mix" of 6.4% is the variable considered for the calculation of the insulation ageing acceleration due to the existence of high frequency transients in the line voltage. The

Table 3.4 – Increase in $\tan\delta$ Compared to Tests with Absence of Transients

Temperature	Increase in $\tan\delta$ (compared with AC only)
$40^{\text{o}}C$	9.88%
$60^{\text{o}}C$	3.35%
$80^{\text{o}}C$	6.00%

"transient mix" issue is solved with an averaged value, not only because of the clear complexity of differentiating the $\tan\delta$ for each temperature and each transient frequency, but also because in the real world the line voltage does not only contain a single frequency transient, but rather a mix of high frequency signals that occur with an unpredictable character and a random set of frequencies.

3.4 Summary and Conclusions

This chapter's main objective was to verify some of the results shown in [9]. By matching the Verification Results with the Original Results, one can posit that the verification was not successful. If we analyse the $\tan\delta$ values for a non-stressed paper sample, the values between both result sets are quite comparable. Nonetheless, all the values obtained by submitting the paper samples to thermal and electrical stresses, turned out to be a mismatch. Moreover, we can also take from table 3.2 that in the Verification Results, the $\tan\delta$ value decreases with the increase of the transient frequency, which contrasts with the behaviour of the Original Results.

There are several reasons that can explain why the Verification Results turned out to be so different than the Original Results, such as:

- a different laboratory operator is sufficient to offset the results, due to the high sensitivity of these $\tan\delta$ measurements;
- although the author tried to reproduce the results by using the exact same set of materials, they have been standing in the laboratory for a period of time that may have altered some of their characteristics;
- the amount of time the laboratory operator takes to handle and transport the sample between the stress site and the measurement site influences the amount of moisture absorbed from the air;
- the fact that only a limited part of the samples survived to the stressing stage (see table 3.3), restrains us from the possibility of outlining behavioural conclusions with much certainty.

Given the verification failure, the author has decided to follow the results posited in [9] that comprehend the following points:

- The $\tan\delta$ decreases in the interval $40^{o}C$ to $80^{o}C$ when a sample is stressed with transients;
- When transient spikes of $1kV$ superimposed on a $2.22kV$ AC waveform are applied in the range from $1kHz$ up to $10kHz$, the $\tan\delta$ increases. The average increase in $\tan\delta$ is 6.4% compared with stressing with $2.22kV$ AC only.

Chapter 4

Framework of Model-Based Optimization

A framework of model-based optimization is hereby presented to allow the usage of intelligent agents in controlling and optimizing the future health state of online network components. As shown before, the components can be subjected to several types of stresses, therefore the presented framework will consider that the cumulative stresses accounted from the various sources can be superimposed and so each one is independent from the other at any time.

Throughout the subsections of section 4.1, an analysis of the necessary framework specifications is performed. We look at how the component's state variables are transformed into readable signals, how to interpret such signals, and the overall specification of a single agent.

The models presented in chapter 2 are applied to the framework in section 4.2, resulting in a complete health prediction model. The applicability of introducing a single agent in a online power component is also studied in section 4.2, with the help of some computer simulations. In these computer simulations, things such as the presence of transients or the estimation precision variation with the increase of the prediction horizon are studied. A comparison between controlled and uncontrolled components is achieved throughout section 4.2, as well.

4.1 Framework Specifications

4.1.1 Estimation of Cumulative Stresses

The estimation of cumulative stresses in the insulation of the transformer is achieved by the use of a group of parallel placed independent signal processing units. A stress estimator, such as the ones listed in chapter 2 is part of each signal processing unit. The idea of such a system is mainly the scalability of the data inputs and therefore the enhancement of estimation's precision. As

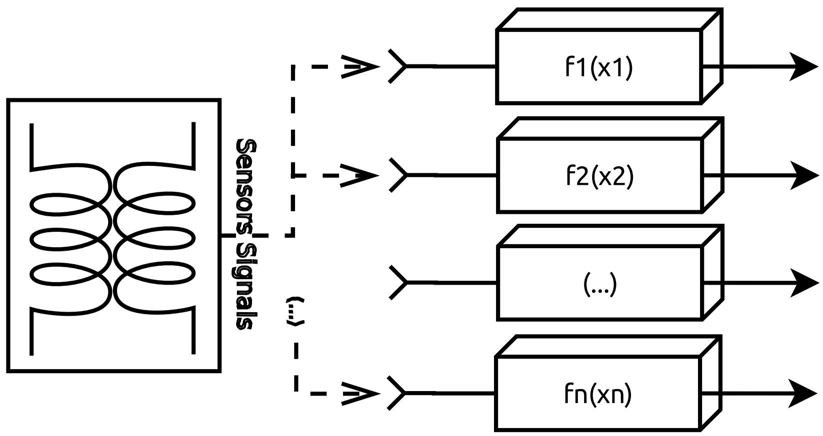

Figure 4.1.1 – Parallel Signals Processing
On the left side, the available sensors read the valuable data from the asset (in this case a power transformer) and push the values into the parallel processing units that compute an output based on the input and the model that is part of each unit.

it can be seen in figure 4.1.1, a variable number of sensors can be installed in the component site (such as a substation), and then a variable number of automated signal interpreters can be used to transform the sensors' readings into absolute stress values that can afterwards be used to compile a global stress estimation of the component.

As stated before, each individual result of the parallel signal processors is considered to be independent from all the others. In this way, not only can we add other signal interpreters regardless of the existing ones, but we can also see each result as an absolute result that will be summed up in order to have, in the end, a value that can be regarded as the total stress inflicted in the insulation of the power transformer. This value is then used by a predictive health model, detailed in subsection 4.1.2, to further analyse the health state behaviour of the component.

4.1.2 Predictive Health Model

The predictive health model interprets the estimations of cumulative stresses inflicted to the component and also the human actions taken to improve the system, such as maintenance (subsection 4.1.3), and computes a prediction of the health state of the component in real time. If the assumption that the input data is constant for a time period of T is taken, then it is possible to predict the health of the component after the time T. With an estimated prediction of the component's health it is possible to automatically, or manually, rethink the management measures taken upon the asset and, not only improve its lifetime usage, but also be ready for and, perhaps, even prevent system failures.

4.1.3 Maintenance

Maintenance actions can be performed on the component, resulting in a reduction of the failure rate - result of the reduction of cumulative stresses. Although it is quite an important factor, its benefits are very difficult to quantify in absolute values. If more data was available regarding the absolute variation of the system health with the occurrence of maintenance, then it would be straightforward to include its contribution in the presented framework. We can consider the maintenance as just another set of the signal processors present in figure 4.1.1 but in this case with positive influence instead of the negative influence that characterizes all the other stress factors.

4.1.4 Agent Constitution and its Applicability to the Power Network

When all the parts of this optimization model come together, a single automated, distributed, and therefore independent agent can be envisioned. Each component of the grid will be part of a set of sub-systems that all together create the system that we call agent. These sub-systems can take into account usage data from the component in question and transform those into valuable data for itself and for the other agents in the network. The other receivers of the agent's outputs can be agents similar to this one, but built upon other grid components, or even a centralized control-action centre. One example of an agent schematics is shown in figure 4.1.2.

In this agent schematics a number of new concepts is introduced. The control-action centre can be considered as the centralized point of control on the utility side, where humans, but also automated systems, monitor the outputs coming from the predictive health model and adjust their management actions in accordance with the agents' indications. The other agents are systems built exactly with the same control and communication set-up. This means that the component itself can be something different than a transformer, as long as the signal processing units and the predictive health model are adapted to the component type. The local planner is an intelligent system that interprets the data locally produced and the incoming data from other automated systems in order to automatically plan actions to be relayed to the actuator. The actuator reacts, not only to internal signals but also to orders that might come from the centralized point of control. It should be noted that, for the agent to automatically take actions based on other agents inputs, it should have a basic knowledge of its surrounding topology.

A simple example of such an automated response would be that Agent A (AA) and Agent B (AB) are both built upon transformers rated at $120^{\circ}C$, transporting energy to the same place, and AA will supposedly reach a temperature of $130^{\circ}C$ within 15 minutes (according to one of the parallel signal processors). AB, which in this example will be at $100^{\circ}C$ in 15 minutes, receives a message that notifies him about the perilously rising temperature of the neighbour

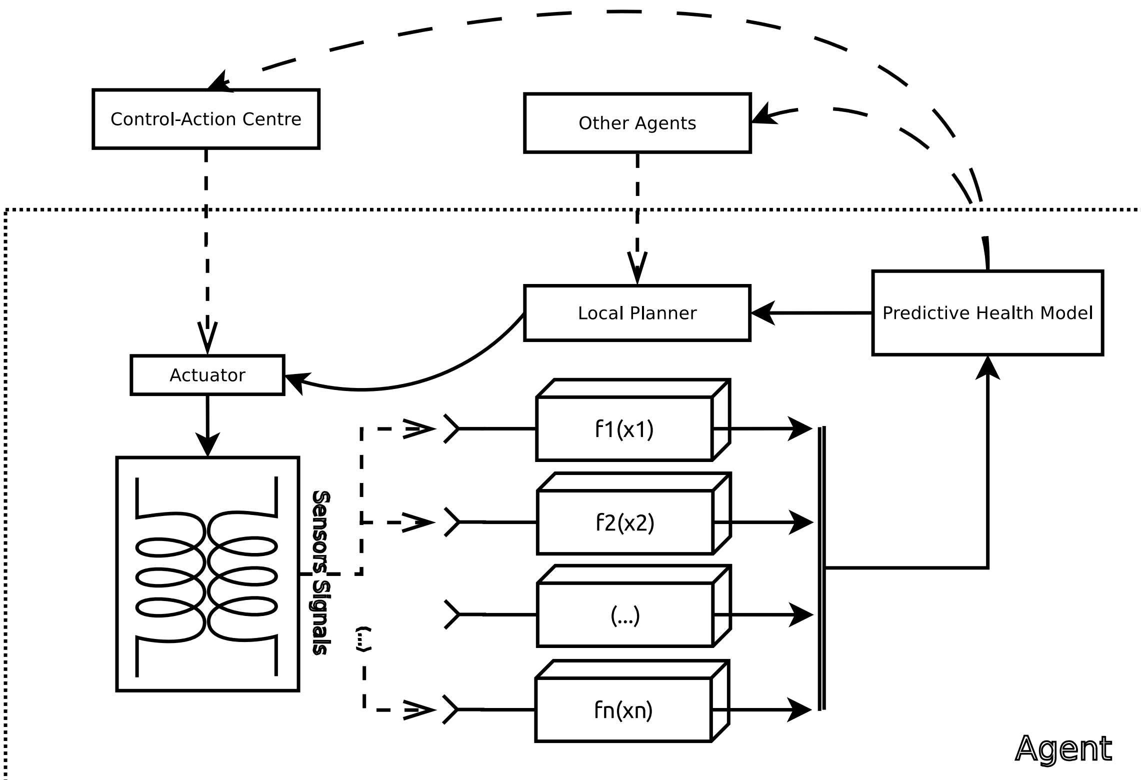

Figure 4.1.2 – Single Agent Schematics
On the bottom the parallel signal processing unit (from figure 4.1.1) sends all the outputs into the predictive health model that merges all the ageing data into a single value that is then locally communicated to the planner and remotely sent to the other agents and, perhaps, a central-action centre.

transformer. Consulting his local database of neighbouring network topology, it is possible for the local planner to ask the actuator to allow more power flow through AB, in order to alleviate the stresses on AA and, not only prolong its lifetime, but also avoid system breakdowns. Simple use-cases as these can perhaps be solved by a smart local planner, but human experience should still be used as a fundamental asset for more complex situations.

4.1.5 Influence of Measurement Errors in Framework Effects

As mentioned before, the calculations performed with the power transformer's thermal models can be replaced by direct measurement through the usage of separate sensors. These sensors can directly measure the Top-Oil temperature, as it is, most of the time, physically accessible. Also, there are sensors that can estimate the Hot-Spot temperature [34]. In this example, we assume that the latter type of sensors is used.

Temperature sensors can both report higher and lower temperatures compared to the real Hot-Spot temperature, so we will analyse error types as plausible conditions. From this point on we will call an error that reports a lower temperature than the real one a negative error. Furthermore, if the error reports a temperature higher than the real Hot-Spot temperature, we refer to it as a positive error.

If we refer to hardware integrity as the main concern, the positive error is not an important condition. The positive error, forces the agent to think that the transformer is in more thermal loading conditions than it actually is. As so, the agent will try to unnecessarily unload the transformer, which results in a decrease of the ageing factor.

The network operator should take more care with the negative errors, as they force the agent to think that the transformer is on a safe thermal loading level and they externally communicate that the transformer can operate more load than it currently does. Depending on the error significance, this type of measurement can easily confuse the agent and make it deteriorate the power transformer.

Taking into account the exponential grow of the ageing factor with the power transformer's Hot-Spot temperature (equation 2.3.2), we can say that the error is more significant for higher values of the ageing factor. As the ageing factor is limited to unity by the agent, we can look at what happens to the system using the unitary ageing factor as a starting point, which is the worst case scenario.

In figure 4.1.3, a plot of the influence of positive and negative measurement errors is sketched. Looking at an expected measurement error of 1% [34] we see that the Positive Error AF is 1.123 and the Negative Error AF is 0.8897. For more extreme measurement errors, such as 10%, the transformer is ageing around 3 times faster than agent believes, due to the Negative Error. On the Positive Error, the transformer is ageing around 70% slower than the initially expected by the agent.

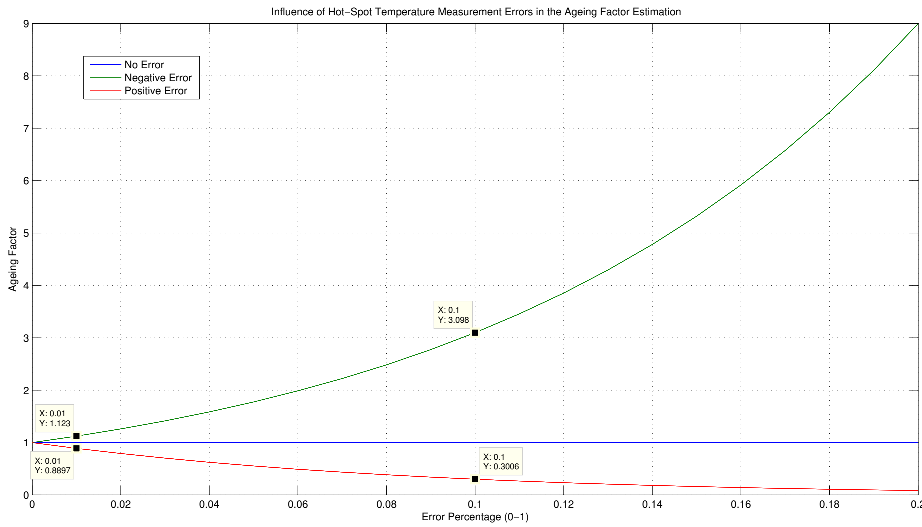

Figure 4.1.3 – Influence of Hot-Spot Temperature Measurement Errors in AF Estimation Positive Error results in a gain in terms of ageing factor, whereas the Negative Error, not only results in a detrimental condition in regard to the power transformer ageing factor, but it also shows a much steeper slope. For an error of 10%, the Negative Error AF is 3.098, while the Positive Error AF is 0.3006.

4.2 Single Agent Simulation - Applicability

To briefly show the applicability of such a framework, a power transformer is equipped with an agent that implements the framework detailed throughout section 4.1. The models to be used are the ones presented in chapter 2. The input simulation data was obtained from a real transformer of the Dutch power network and it is a dataset composed of the power flow values for one whole day. The shape of the waveform fits the usual electricity daily usage curve and can be seen in figure 4.2.1. The highest power flow occurs around the evening period.

4.2.1 Specifications

For this simulation, an example power transformer is taken into account with the parameters from table 4.1.

According to the suggestions from IEEE C57.91 [4], the recommended hot spot temperature to achieve a normal life expectancy loading is about $120^{\text{o}}C$, and therefore, during this simulation, the maximum allowed hot spot temperature will be $\theta_{hs,max} = 120^{\text{o}}C$. We take this value as the maximum temperature of the power transformer windings, because this is the only stress factor being accounted for. This means that if $\theta_{hs} = 120^{\text{o}}C$ then $FAA = 1$, being the latter the key

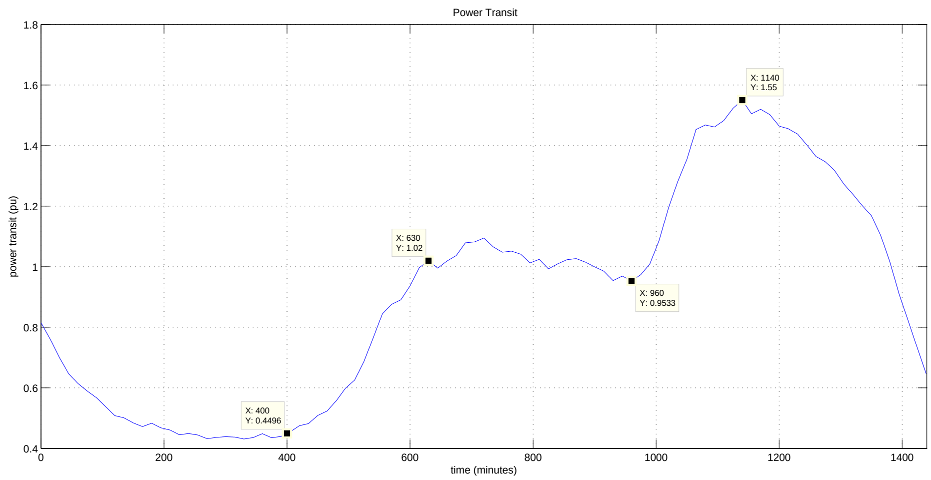

Figure 4.2.1 – Load Shape of a Day on a real Node of the Dutch Power Network

On a real day in this point of the network, the load starts by descending from midnight onwards until it hits a minimum at around $4h$ ($240mins$). The load starts increasing from around $6h30$ ($\pm 400mins$) until $10h30$ ($630mins$) when it stabilizes until almost $16h$ ($\pm 960mins$). From that point on there is an increase of load that peaks at around $18h30$ ($\pm 1140mins$), where it reaches $1.55pu$. After the peak, the load decreases again until the end of the day.

Table 4.1 – Parameters of the example power transformer, from an example in [7].

Details about these variables, can be found in section 2.2. It can be said that the initial hot-spot and top-oil temperatures are set to be $38.3^{o}C$, which shows that the power transformer is far from the rated operation point. Moreover, it is important to set the initial temperatures in a way that the hot-spot temperature is always higher or equal to the top-oil temperature, to ensure a model restriction (2.2).

Transformer Parameters		
$\theta_{oil,rated} = 75^{o}C$	$\tau_{wdg,rated} = 6min$	$P_{cu,dc} = 411780W$
$M_{FLUID} = 73887kg$	$P_{cu,eddy} = 29469W$	$P_s = 43391W$
$R = 1000$	$\Delta\theta_{oil,rated} = 38.3K$	$\Delta\theta_{hs,rated} = 20.3K$
$\theta_{oil,i} = 38.3^{o}C$	$\theta_{hs,i} = 38.3^{o}C$	$n = 0.25$
	$\theta_{hs,rated} = 120^{o}C$	

objective. In the case of existence of other stressing factors, such as in section 4.2.2.4, then we look just at the $FAA = 1$, which means that the $\theta_{hs,max}$ will have to be lower than 120ºC.

As the only available input data is the power flow of the transformer during $24h$, we will make use of the thermal model show in section 2.2 to estimate the top-oil and hot-spot temperatures of the component in real-time. The results from chapter 3 will also be included in this simulation. These two aforementioned results will be the input signals of the predictive health model module (that can be seen in figure 4.1.2). The ageing models discussed in section 2.3 and the influence of the existence of transients discussed in chapter 3 are to be used in the predictive health model module.

The simulations that will take place in section 4.2.2 include a comparison between the usage of the described control systems and its absence. Factors like the existence of transients will also be varied, in order to evaluate its global influence in the system.

4.2.2 Example Simulations

As mentioned before, different types of data that can originate from different simulation set-ups. Throughout this section, different types of stresses and different model parameters will be tested.

4.2.2.1 Uncontrolled Hot-Spot Temperature

A transformer is placed in the point of the network where the waveform depicted in figure 4.2.1 will be the load that should pass through it. In an uncontrolled system, all the load is transported by the transformer. The resulting temperature figures are shown in figure 4.2.2. This figure shows that the hot-spot temperature is higher than the rated temperature for almost 200 minutes, which according to section 2.3 significantly harms the component, as the insulation ageing acceleration factor rises exponentially with the hot-spot temperature.

4.2.2.2 Controlled Hot-Spot Temperature

In the case of a controlled agent, the results are quite different. In the current simulation system, basically if the hot-spot temperature is expected to be higher than the rated temperature, then the excess power flow is rerouted. How excessive power is rerouted will be discussed in the next chapter. The results of a simulation that restricts the hot-spot temperature to, in this case, 120ºC are shown in figure 4.2.3.

As a result of the controlled temperature system, for each time step in the simulation[1] a maximum allowed power flow is calculated, based on the thermal models shown in section 2.2, and represented in figure 4.2.4 as the red line. It can be seen that, as expected, the lower the

[1] The simulation step is, in this case, 1 minute

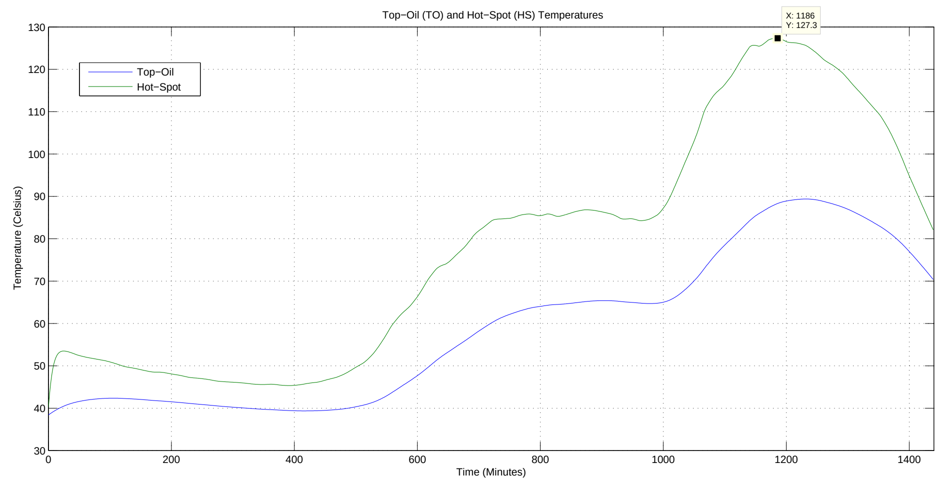

Figure 4.2.2 – Simulation of an Uncontrolled Component
Given the load profile from figure 4.2.1, the top-oil and hot-spot temperatures are computed with the previously mentioned thermal models. The hot-spot temperature is the green curve which always shows higher temperature values, while compared to the top-oil curve. The maximum temperature of this plot - $127.3^{\text{o}}C$ - is reached at the minute 1186. This peak value is registered a bit after the peak of the power flow, due to the cumulative behaviour of these models.

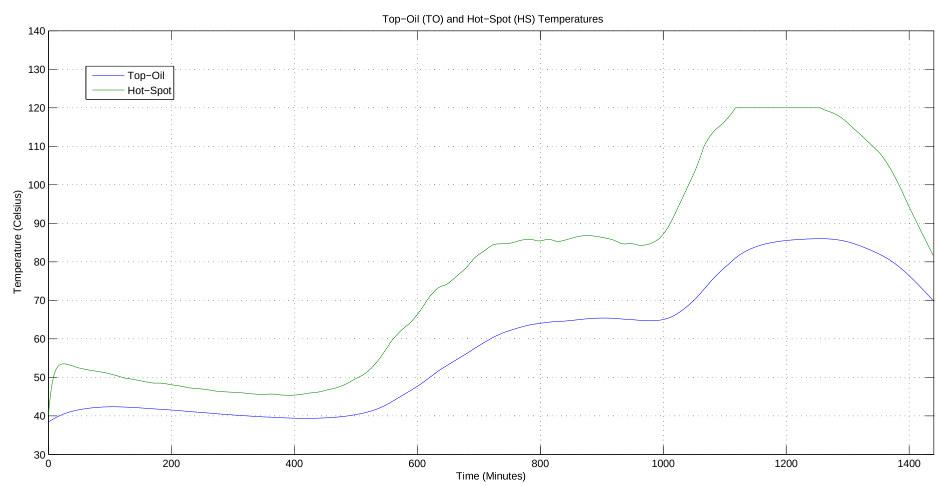

Figure 4.2.3 – Simulation of a Controlled Component
The component is subjected to the wave form show in figure 4.2.1, but there is a control method that shapes the load whenever the hot-spot temperature is expected to be higher than $120^{\text{o}}C$ on the next step. This results in the horizontal surface observed between the interval $[\pm 1100; \pm 1250]$.

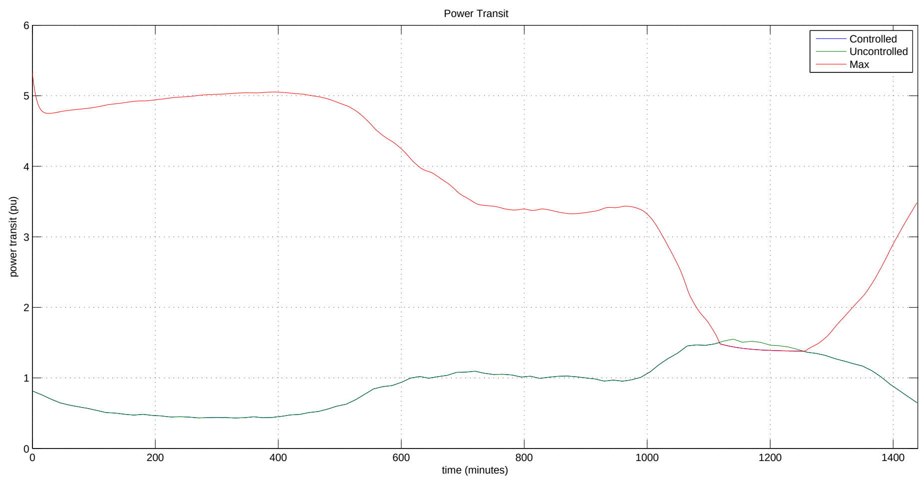

Figure 4.2.4 – Power Flow of a Controlled and an Uncontrolled Components
The green curve shows the power flow that will be transmitted by the transformer in the absence of control methods. The blue curve shows the power transmitted by a controlled transformer and the red curve shows the maximum possible value of transmitted power given the current transformer temperature. When both blue and red curves match, then the load has to be shaped.

temperature of the transformer, the more power can be carried by it in the next simulation step. After around minute 1100, the hot-spot temperature reaches the $120^{o}C$ threshold and therefore power has to be rerouted.

In the detailed view of figure 4.2.5, it can be seen that the controlled wave is always below the maximum calculated power flow. The difference between the controlled and the uncontrolled wave is the rerouted power. In this example simulation, the total power transit over the full day is $1307.1pu$ and the amount of power that has to be rerouted is only $10.24pu$. This means that, in order to keep the temperature below the rated temperature, in a situation where the uncontrolled case would make the temperature to be over the rated temperature for about 200 minutes, only $\frac{10{,}24}{1307{,}1} \times 100 = 0.78\%$ of the total power needs to be rerouted.

4.2.2.3 Controlled versus Uncontrolled Hot-Spot Temperature

The current simulation set-up can be further used to produce other types of data, like the calculation of an ageing factor in real-time and its contribution to an absolute value of lifetime loss of the component. In the current subsection, a comparison is made between a controlled and an uncontrolled component. In terms of temperature variations, a clear image can be taken from figures 4.2.2 and 4.2.3. A comparison of the uncontrolled power flow and the controlled version with its corresponding rerouted power was also already compiled in figure 4.2.5. In figure

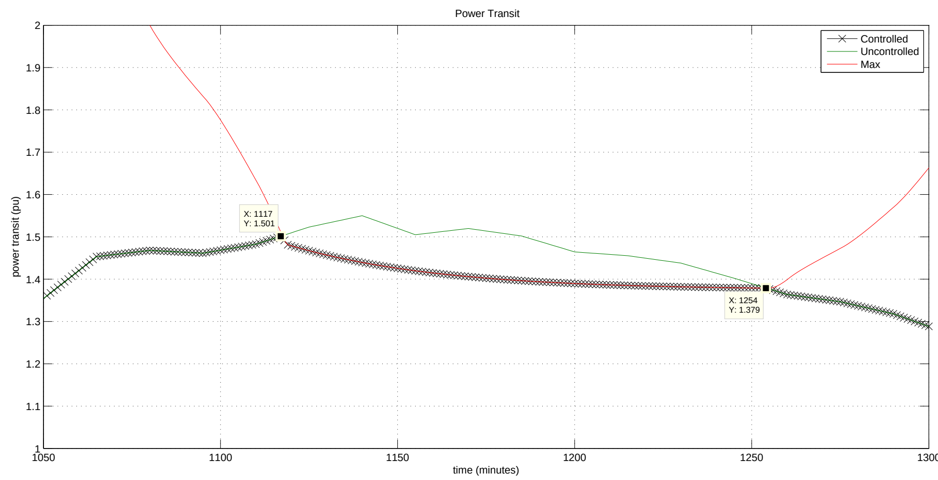

Figure 4.2.5 – Power Flow of a Controlled and an Uncontrolled Components - Detail View
This is a detailed view from figure 4.2.4 in the area where the load is shaped. It can be seen that the controlled power flow can never be higher than the maximum power flow and that is the reason why the load is shaped between minute 1117 and 1254.

4.2.6, the ageing factor is calculated by using equation 2.3.2. Although the rise of the hot-spot temperature in the uncontrolled component is quite brief and does not seem to be significant[2], its consequence on the ageing factor is very powerful. The highest peak of ageing factor on the uncontrolled component reaches a value higher than two, whilst the highest value of the controlled agent is specified to not go any higher than one.

As the ageing factor, in the controlled agent, never reaches a value higher than one, the component ages slower than estimated by the manufacturer. Consequently, the component's available lifetime can be considered as extended. These ageing factors can be transformed in real lifetime loss in minutes as stated in equation 2.3.3. The comparison between the Lost Life Time (LLT) of both components in test is achieved by summing up the minutes of lost life time plotted in figure 4.2.6. The controlled method results in an absolute ageing of 260 minutes and the uncontrolled method results in 371 consumed minutes.

In the above case, considering the fact that the total duration of the simulation is 1440 minutes, it can be noted that the total LLT of the controlled agent is about 18.07%[3] and the one from the uncontrolled component is 25.74%[4]. If we compare both values, the uncontrolled component LLT is about 42.43%[5] higher than the one from the controlled agent case.

[2] The highest peak of temperature is only $\frac{127.3^oC - 120^oC}{120^oC} \times 100 = 6.08\%$ higher than the rated temperature

[3] $\frac{260.2}{1440} \times 100$

[4] $\frac{370.6}{1440} \times 100$

[5] $\frac{370.6 - 260.2}{260.2} \times 100$

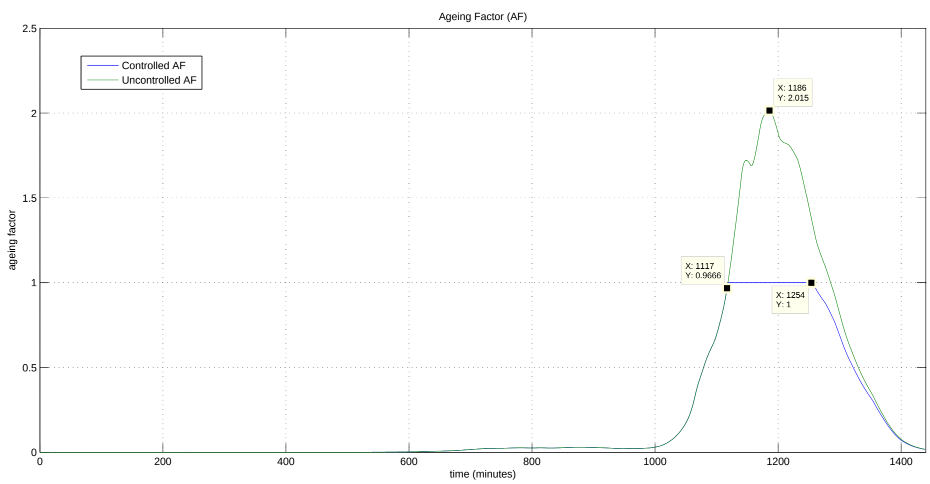

Figure 4.2.6 – Ageing Factor Comparison

The curve that refers to the controlled component (blue) is shaped ($[1117; 1254]$) such as the load curve. The maximum ageing factor allowed is 1, that corresponds to the rated hot-spot temperature of $120^{\circ}C$. In the green curve, the acceleration ageing factor peaks at the 1186 minute (where the temperature also peaks on figure 4.2.2), by reaching the value 2.015. This means that, at that point, the insulation of the transformer is ageing at a rate around twice as much as it was planned for.

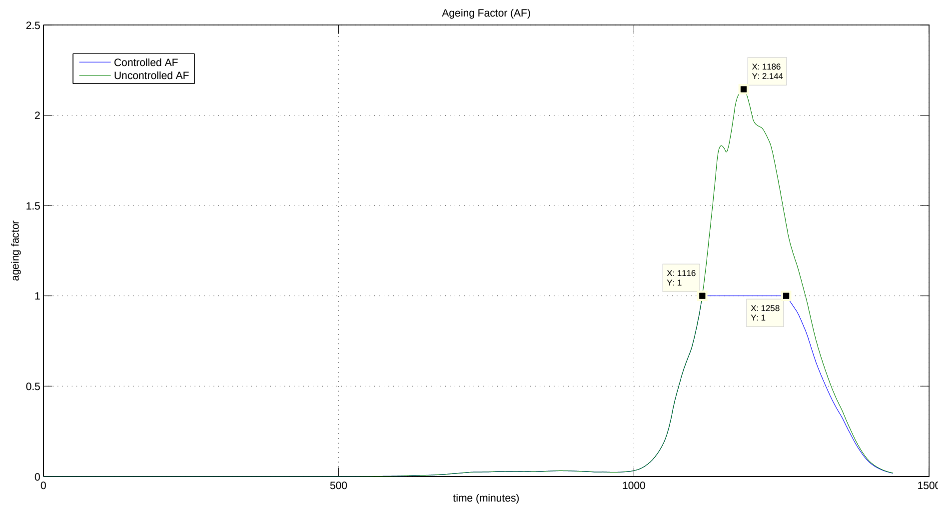

Figure 4.2.7 – Ageing Factor Comparison - High Frequency Transients

The presence of high frequency transients increases the accelerated ageing factor by 6.4% and that results on larger deterioration of the component, while compared to figure 4.2.6, where there was no presence of high voltage frequency. The curve that refers to the controlled component (blue) is shaped such as the load curve. The maximum ageing factor allowed is 1, that, in this case, does not mean a temperature of $120^{\circ}C$, due to the presence of transients. In the green curve, the acceleration ageing factor peaks at the 1186 minute (where the temperature also peaks on figure 4.2.2), by reaching the value 2.144. This means that, at that point, the insulation of the transformer is ageing at a rate around twice as much as it was planned for.

4.2.2.4 Presence of High Frequency Transients

If all the other simulation inputs are maintained, the presence of high frequency transients, according to chapter 3, can cause an average increase of 6.4% in the total FAA of the component. In the last few examples, the limiting factor was always $\theta_{hs,max} = 120^{\circ}C$, because the temperature was the only value affecting the insulation lifetime (as the thermal model was the only one being used by the optimization framework). In the presence of high frequency transients, the framework now reads two different stress factors, which means that not only the temperature contributes to the increase of the FAA, but also the high frequency transients affect its behaviour with an increase of 6.4%. In the end, for this example we need to limit the FAA value to 1.

As expected, the inclusion of high frequency transients will detriment the system's behaviour while compared to the last subsection's, as shown by figure 4.2.7.

While summing up the minutes of lost life time plotted in figure 4.2.7 we come up with the result that the controlled method generates an absolute ageing of 266.1 minutes and the uncontrolled method generates 394.3 consumed minutes.

In this case, the total LLT of the controlled agent is about 19.22%[6] and the one from the uncontrolled component is 27.38%[7]. If we relate both values, the uncontrolled component LLT is about 42.45%[8] higher than the one from the controlled agent case.

4.2.2.5 Variations of the Prediction Horizon

All the previous simulations were performed with an prediction step of one minute, meaning that every minute the predictive health model evaluates what the transmitted power should be to make sure the rated temperature is not exceeded. On one hand, the smaller the prediction step is, the more frequently an evaluation is done and therefore a better control of the component's health state is achieved. On the other hand, the more frequently these computations are performed, the more computational power is needed and a larger amount of data has to be handled. To avoid this, a compromise between a good estimation (low prediction step) and a low computational need (high prediction step) has to be taken.

In this section, the prediction step value is changed in order to better understand what its influence is in the performance of the agent as a system.

In figure 4.2.8, one can see a simulation with a prediction step of 15 minutes. In this case, the amount of rerouted power is $14.72pu$, that is 1.13%[9] of the total power transported by the component on the uncontrolled situation.

If we increase the prediction step to once per hour (60 minutes), the result is noticeable different, as it can be seen in figure 4.2.9. In this case, where the prediction horizon is 60 minutes, the total rerouted power is $68.91pu$ which is already 5.27%[10] of the total power of the whole day in the uncontrolled simulation.

From figure 4.2.4, it can be calculated that the total rerouted power is only $10.24pu$, which is only 0.78%[11] of the total power.

A summary is compiled in table 4.2, where it can be seen that for a higher prediction horizon, the amount of power that needs to be rerouted is also higher, causing more disturbances in the electrical system as a whole. Moreover, it is interesting to note that a higher prediction horizon not only does not increase the lifetime consumption of the component, but even decreases its lifetime consumption, since more power has to be rerouted through other devices. If we look at the agent itself and assume that re-routing power through other devices is a feasible and harmless task, then a higher prediction interval would be nothing but beneficial. Considering

---

[6] $\frac{276.8}{1440} \times 100$
[7] $\frac{394.3}{1440} \times 100$
[8] $\frac{394.3-276,8}{276.8} \times 100$
[9] $\frac{14.72}{1307.1} \times 100$
[10] $\frac{68.91}{1307.1} \times 100$
[11] $\frac{10.24}{1307.1} \times 100$

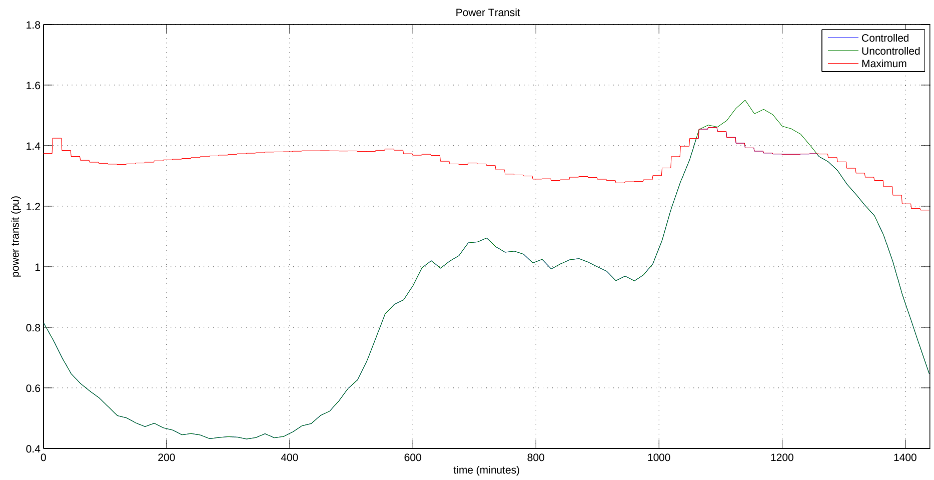

Figure 4.2.8 – Power Flow of a Controlled Component - Prediction Step of 15 minutes
The maximum allowed power flow is computed every 15 minutes, instead of the previously shown 1 minute prediction step. The area between the red and the green curve, when the red curve is below the green one, is the rerouted power flow.

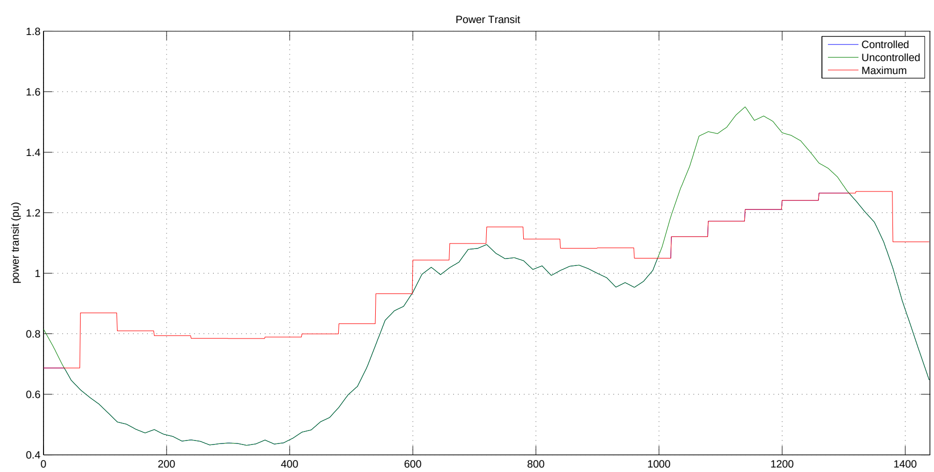

Figure 4.2.9 – Power Flow of a Controlled Component - Prediction Step of 60 minutes
The maximum allowed power flow is computed every 60 minutes, instead of the previously shown 1 minute prediction step. The area between the red and the green curve, when the red curve is below the green one, is the rerouted power flow.

Table 4.2 – Influence of the Prediction Interval on Rerouted Power Flow

Prediction Horizon (min)	Rerouted Power (%)
1	0.78
15	1.13
60	5.27

this, we can state that an increase of the prediction horizon is computationally beneficial to the agent itself, but it raises issues on the network management level.

The ideal value for the prediction horizon is, therefore, not only dependent on the computational power available, but mostly on the surrounding network capacity to accept more power. If all the neighbouring transformers are overloaded, then a computational effort has to take place, in order to decrease the prediction horizon and decrease the rerouted power.

4.3 Summary and Conclusions

Each one of the agents reported in this chapter is a set of layers added on top of a power network component. These agents can be used to simply read data points of the component's health status, as seen in all the uncontrolled example simulations. Nonetheless, the key interest is in enabling these agents to actively make use of the readings on the go to actuate the component's adjustable sub-systems, such as the tap changers in the case of a power transformer.

- By building an agent on top of a power transformer, it was shown in section 4.2.2.3 that it is possible to reduce the lifetime loss by more than 40%, by rerouteing only 0.78% of the total power through the transformer. This result was achieved with a simulation prediction horizon of 1 minute.
- In order to reduce the necessary computational power and network bandwidth, one can increase the prediction horizon, which results in less computed data and therefore less transmitted data. This better computational result, has a detrimental effect over the amount rerouted power to maintain the temperature under the rated value. For prediction horizons of 15 and 60 minutes, the rerouted power for the same simulation is 1.13% and 5.27%, respectively.
- Regarding the inclusion of high frequency transients in the simulation waveform, the incremental factor of 6.4% over the FAA causes the controlled system to start rerouteing power 1 minute earlier and it only stops rerouteing power 4 minutes after the example with no high frequency transients. Furthermore, one can see that the lost lifetime is about

2.27%[12] and 6.4%[13] higher in the controlled and uncontrolled simulations, respectively, while comparing the high frequency scenario to the previous one.

- In the controlled case, the increase of the LLT, due to the introduction of high frequency transients, is not as large as the uncontrolled case, because the FAA variation with the hot-spot temperature is not a linear relation, as it increases faster for larger temperatures. This means that in the uncontrolled simulation, the "transient mix" causes more damage than in the controlled scenario.
- Thermal estimations can be replaced by online sensors that report temperature values that might contain errors. The system's sensitivity to these errors can be divided in two branches: positive and negative errors. Regarding hardware integrity, the most significant error to be studied is the negative error. For expected measurement errors of up to 1% the transformer can age up to 12% faster than expected. For larger errors, that would probably be the output of a broken sensor, the power transformer's integrity can be highly compromised, as it can age up to 3 times faster for an error of 10%. Although this fact seems to compromise the system, the same if true for human operated networks, as the operators will also take actions based on sensors outputs. A set of reality checks have to be performed by both humans and agents in order to achieve an architecture more independent from errors in its input signals.

[12] $\frac{266.1-260.2}{260.2} \times 100$
[13] $\frac{394.3-370.6}{370.6} \times 100$

Chapter 5

Introduction of Agents in the Electrical Power Grid

The integration of smart agents in the electrical power grid can be, as will be shown throughout this chapter, highly beneficial but it also triggers several issues that need to be targeted. The major issues, such as grid topology, predictive health system topology, security, stability, communications, synchronism, and computational power, are also addressed in this chapter. The first problem to look at is the topology of the predictive health system, on which all the other issues are dependent. There are two main possibilities for how to make use of the predictive health model: centralized or decentralized action control. On both topologies, the idea is to place one agent in each component of the power grid and let it communicate with the outer world in order to achieve a better usage of the available resources in the electrical grid. The usual power flow calculation looks at the distance between buses and the cost of generation. In this chapter, a careful look at the health states of each power transformer is also conducted. Example simulations can be found throughout the chapter, always regarding the well-known IEEE 14 bus network (figure 5.0.1). These example simulations include a centralized computation network that has the predictive health model running on each agent and informs the network operator about the current and predicted health states of the system assets and also a decentralized simulation that not only has an online predictive health model, but also runs a decentralized automatic action control procedure, by allowing communications amongst groups of agents and actions on the assets variables.

On both discussed topologies, the included agents perform by making use of two different calculations: one with a time step of 1 minute and another with the time step of 30 minutes. By doing so, at each minute, all agents can compile an output with the current accelerated ageing factor and the one that is expected to occur in 30 minutes.

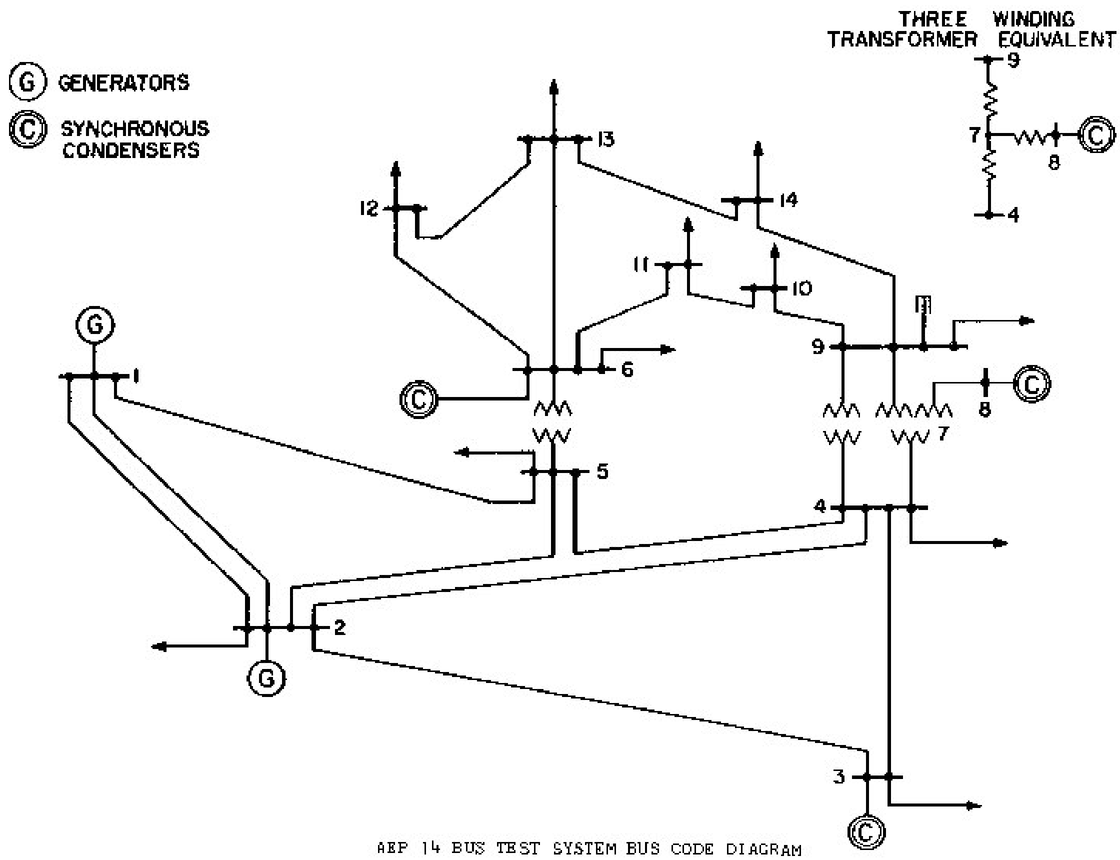

Figure 5.0.1 – IEEE 14 bus test network diagram
Generation is on the bottom side of the network and most of the load points on the topmost side. Three transformers are part of this network.

Throughout section 5.1, a centralized action-control point is discussed, by detailing most of the key challenges and advantages within such paradigm. The control action is left for Human agents, and therefore, not performed in the presented simulations. Moreover, in section 5.2, not only the topology of the communications network is built around a decentralized control perspective, but also as the control action is to be performed by the automated agents.

A comparison between both paradigms regarding possible cost reductions can be found in section 5.3.

5.1 Centralized Action-Control Point

A centralized health predictive control point basically means that every agent sends the result of its calculations to a central control unit point in which the decision making takes place. The outcome of the decision is sent back to each agent as an order that will be applied by the actuator inside the agent's structure (figure 4.1.2). The decision-making can be a manual or an automatic process. This means that, topologically, one major difference between the existing network configuration and the one proposed is the existence of smart agents in each transformer and the means of communication that ensure the health prediction of each agent reaches the utility/control-action centre and that the action from the utility based on the input of the agents gets to the right actuators in order to maintain the stability and the resource efficiency of the network.

5.1.1 Communication

From a centralized decision-making perspective, one needs to ensure that all the data computed in the agents reach a central, and perhaps distant, point of the network. At this point, an actor, such as a human or an automated system, performs data-mining with the objective of outputting a set of actions that will maintain or even restore the stability of the network.

5.1.2 Synchronism

Assuming that a central point is collecting and processing all the data, a considerable effort has to be done regarding the synchronism of the incoming data sets. For every time step, each agent sends one data package to the central point. Ideally, in order to be able to compute a representative result, all the data packages coming from the different agents at the same time need to regard exactly the same step in time, so that the action is only taken after the acknowledgement of the whole system status at that time. There are two cases where this ideal scenario does not happen: if during time step T there is a missing data package or if during the same time step T there is an extra data package from $T \pm 1$. In both cases, at the end of the time step, the computation should still take place. In the first scenario, the computation will ignore the absence of the data package and be executed with the available data. It might be the case that the missing reported value is from a highly loaded power transformer and the result action request from the decision making centre (with no access to such information) can detrimental towards this out of sync agent. In the second scenario, the computation process has to ignore the extra value, as it does not represent the system at the ongoing time step and might generate inadequate results.

These synchronism issues could play a key role if the simulation step was intended to be a very small amount of time, like μs. In this case, the step value we are aiming for here is in the order of one minute, making it easier to converge the agents into synchronism. As long as all the packages arrive at the decision-making centre within one minute, then the whole process should be successful, synchronism-wise. This does not mean the network operator can skip the planning actions and the monitoring effort for syncing the agents, although the margins are much safer than with a μs time step.

In order to achieve synchronism and also to evaluate whether it has actually been achieved, all the packages need to be timestamped. In this way, it is also possible to evaluate at the receiver side whether a certain received package fits the current calculation window. In the case that one of the packages does not belong to the group, that package should be dropped, to avoid faulty decisions.

On the agent side, it is also necessary to have an input verification system that matches each decision coming from the central computation point to a single sent message, by matching their timestamps. This extra step also ensures that the agent does not lose sync with the central decision-making unit, which being in sync with all the other agents also ensures that the agents are in sync with each other without direct contact between them.

5.1.3 Computational Power

The demand of computational power is mostly dependent on the number of layers present in the agent. As formulated in chapter 2, there is a large number of models that can be useful to predict the health state of the system under consideration. The larger the number of models and its complexity, the larger the required online computational power will be. Even if we only include the predictive health model detailed in 2.3, if the agent also includes temperature sensors for the top-oil temperature, it is already one less computation that needs to be executed every cycle. Minor calculations like these can make a significant computational difference, if they are a relatively large part of the whole process.

At this point, it is difficult to elaborate on the necessary computational power per agent, but it can surely be said that for calculations happening every minute, the number of models in the framework has to be quite significant for the need of computational power to be noteworthy. As an example, it can be said that in one minute, a regular household computer processor can compute 105339025 times[1] the equations shown on chapter 2. Regarding this example, it becomes clear that the number of models plugged into the framework need to be large for the computation to be a problem.

5.1.4 Practical Implementation and Results

Assuming that all the non-electrical issues are solved and we can successfully equip every power transformer in the network with a predictive health control agent, then we can start off by simulating the well-known IEEE 14 power network shown in figure 5.0.1 that has in its composition three power transformers, being one of them a three winding transformer. As this network's specifications offer only fixed loads, in order to proceed with testing, we carry on using the waveform previously shown on figure 4.2.1 by applying it on one of the nodes of the IEEE 14 bus network, creating one disturbing node and leaving all the others exactly the way they were planned to be in the network specifications.

In a real case scenario, the power flow through the transformers would most likely be measured by sensors and those values could then be used to feed the prediction health control system. In this specific case, due to the absence of such data, a power flow calculation has to be done for each step. This should be regarded as extra computation, as it is unnecessary in the real world application. Given so, we will make use of the open source power flow calculation tool written in MATLAB, MATPOWER [12]. In the current simulation scheme, the agents will be loaded with the same initial data as given in section 4.2 and the one day load shape shown in figure 4.2.1 will be placed on the node number 13. This load shape is multiplied by a factor, in order to contextualize the load to the current network scenario. By doing so, the load on node 13 is much higher than the one the network was planned for. With a quick look at the network and at its topology, it is straightforward that, given a high load on node 13, the most stressed transformer is the one that connects buses 5 and 6.

5.1.5 Simulation with Agents without Control

To compute this simulation, agents have been placed in each power transformer of the network. Each agent has a local database of state values and uses it, not only to provide other network entities with valuable data, but also to be able to compute the next step of the simulation, as the models are mainly discretized differential equations and therefore need the current system state in order to build the next estimation. In the case of no control action, these values are used to be sent to the control centre for information purposes only. In the current simulation, not only the next step (1 minute) is calculated, but also a prediction of thirty minutes is computed, by increasing the step size as previously shown.

[1] tested on Intel® Core™ i5 CPU M 480 @ 2.67GHz × 4, using one core only

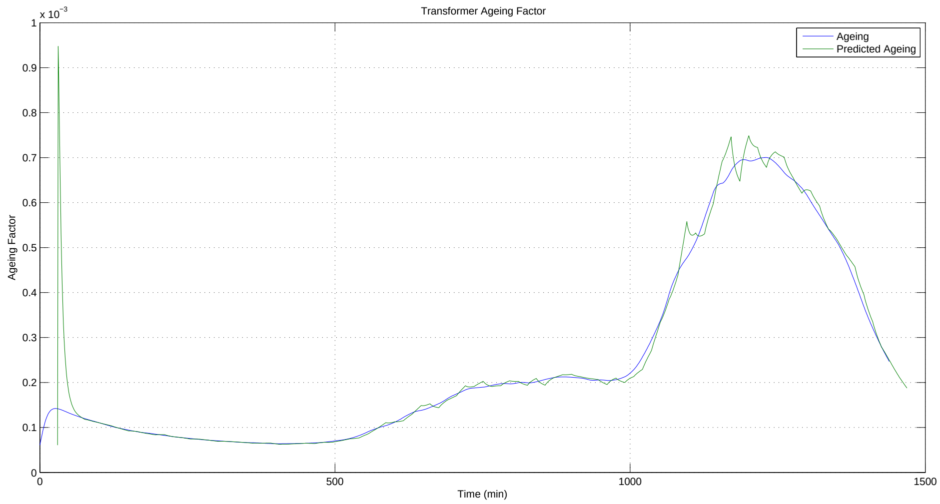

Figure 5.1.1 – Ageing Factors of Transformer 4 to 7
The blue curve is a computation of the transformer ageing factor in real time and the green curve is a computation of a 30 minutes prediction. The initial peak in the green curve is a result of the steep increase of the hot-spot temperature shown in figure 4.2.2. The peak is so visible because the model assumes that the increase of the hot-spot temperature will be steady over 30 minutes.

By simulating the mentioned electrical network during one day (1440 minutes) with a higher load on node number 13, by applying the load of figure 4.2.1 multiplied by a factor[2] of 1.7, and assuming all transformers exhibit equal thermal behaviour, the results present in figures 5.1.1, 5.1.2, and 5.1.3 are generated.

In each one of the resulting simulation plots, one can identify two curves. The blue curve draws the ageing factor of the transformer during the day calculated every minute with steps of one minute. The green curve is an estimation of 30 minutes ahead of the current time. This means that the predicted ageing values are also calculated every minute, based on the current state values of the transformer, but the step of the estimation is of 30 minutes instead of only 1 minute. This causes an increase in the prediction error, but it creates a very useful opportunity to take an early action against possible harsh undesirable ageing factors.

Given the results shown in figures 5.1.1, 5.1.2, and 5.1.3, it is clear that the high increase of load on node 13 resulted in a enormous stress in the transformer that connects nodes 5 and 6.

[2]as previously stated, in order to contextualize the example load with this network, we have to scale up the load profile. The multiplication factor of 1.7 is the value that is high enough to place the transformer between nodes 5 and 6 on a delicate situation in which a quick increase of load on node 13, directly causes a significant perturbance in the mentioned transformer.

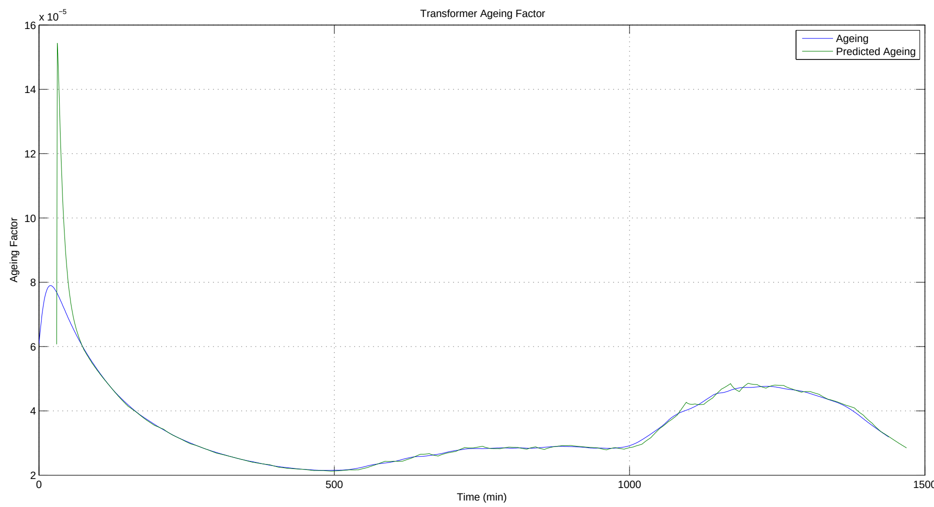

Figure 5.1.2 – Ageing Factors of Transformer 4 to 9
The blue curve is a computation of the transformer ageing factor in real time and the green curve is a computation of a 30 minutes prediction. The initial peak in the green curve is a result of the steep increase of the hot-spot temperature shown in figure 4.2.2. The peak is so visible because the model assumes that the increase of the hot-spot temperature will be steady over 30 minutes.

Table 5.1 – Simulation Summary

Transformer	Ageing (mins)	Pred.Ageing (mins)	Error (mins)	Error (%)	Power (pu)
4-7	0.22568	0.22901	0.00333	1.476	267.3618
4-9	0.018252	0.018371	0.000119	0.651	152.2114
5-6	457.5314	490.1913	32.6599	7.138	585.7481

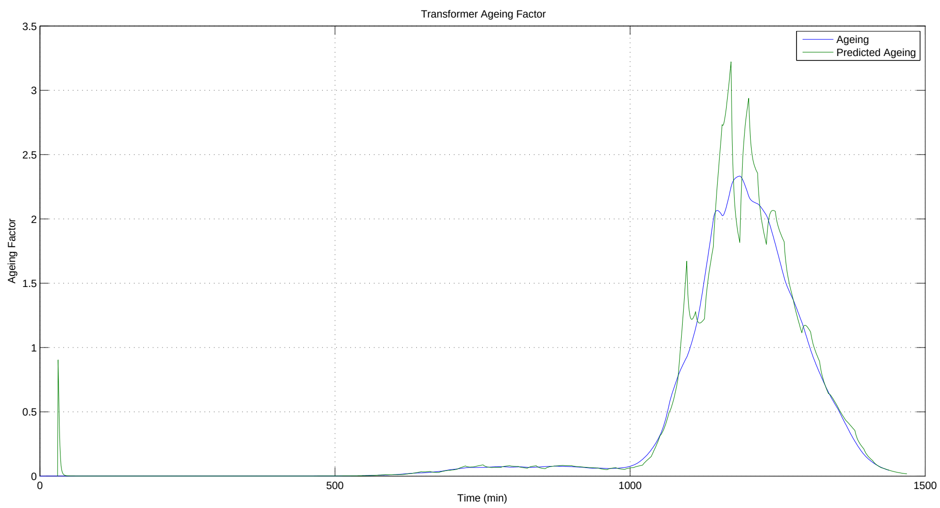

Figure 5.1.3 – Ageing Factors of Transformer 5 to 6
The blue curve is a computation of the transformer ageing factor in real time and the green curve is a computation of a 30 minutes prediction. The initial peak in the green curve is a result of the steep increase of the hot-spot temperature shown in figure 4.2.2. The peak is so visible because the model assumes that the increase of the hot-spot temperature will be steady over 30 minutes.

From all the power transported from the generation side[3] into the consumption side[4], most of it was transported by the transformer that connects nodes 5 and 6 and that is the reason why the transformer is considerably thermally overstressed.

Several observations can be taken from table 5.1 and figures 5.1.1, 5.1.2, and 5.1.3:

- There is an enormous difference among all transformers, regarding insulation ageing. If we compare the transformer 4-7 against the 5-6 there is an increase of around 200000%;
- The transformer 5-6 shows an increase of transported power of only 119% when compared to the 4-7 transformer;
- It is also worthwhile to look at the error that arises from the prediction of the ageing factor 30 minutes ahead of time, as it it only around 7% in the most significant case. Looking at the figures, one can see that both curves (the current and the predicted one) follow each other quite steadily. Given so, in this simulation, it seems to be a wise approach to use the 30 minutes as the prediction step.

With this simulation and in the absence of any control action to reduce the load on the branch 5-6, it is clear that the power flow analysis using the usual methods of reducing the ohmic losses and balancing the cost generation to make better use of the existing network resources fails to achieve its objective. However if the ageing prediction factors reach a control centre or if they trigger an automatic decentralized action to reverse the tendency of the power flow to try to go through the branch 5-6, by taking into account the assets ageing as a cost variable and rerouteing some of the power through the other two transformers, the results will clearly improve.

It must be emphasized that the prediction interval of thirty minutes creates the possibility of early control methods even if they are performed by human agents in a centralized fashion. As an example, one can note from figure 5.1.3 that around minute 1050, the predicted ageing factors were already around 1.7, while the actual ageing factor was still lower than 0.3. This predicted dramatic increase of ageing factor should, by minute 1050, be already considered an emergency situation and some power rerouteing measures must be taken. As previously shown, this prediction interval can also be increased, but then its accuracy will be lower and may be compromised as a reliable indicator.

5.2 Decentralized Action-Control

A decentralized action-control system can be achieved while reusing the agents concept previously shown in figure 4.1.2, by making the agents communicate with each other and, with local

[3]we consider the generation side the bottom part of figure 5.0.1, including nodes 1, 2, 3, 4, and 5

[4]the consumption side of the network is considered to be the upper part of figure 5.0.1, that includes nodes 6, 7, 8, 9, 10, 11, 12, 13, and 14

computation, enable them to make decision and perhaps, based on that, even take actions. This idea raises quite some challenging issues that are constantly addressed in decentralized systems in general, but it also raises some electrical network specific issues. The topics addressed in section 5.1 will be referred as well in this section, so that we can build up a reasonable comparison between both paradigms. It should be noted that this decentralized system should be able to overlap with the existing centralized system, so that both can coexist, at least until all the network control is also applied in a decentralized fashion.

5.2.1 Communication

As previously stated, all agents need to be able to communicate with each other, in order to enable them to make decision and perhaps take actions. As so, all the communication channels have to allow input and output possibilities. Due to the self-healing nature of wireless communications [34], a wireless network is the ideal solution for these local communication channels, in order to diminish the possibility of critical points of failure.

Due to the large importance of the electrical network, allowing an agent to receive data from other agents, has to be a very sensitive measure. A major emphasis has to be granted to the security of this type of communications. The communications between the agents should all be encrypted with a pair of keys, one from the sender and one from the receiver, so that only the receiver can open it and only the sender could have sent it. All the agents need to have an internal database with, not only all the agents they can talk to, but also their respective security keys. In this way, we ensure that no hacking is possible from external entities.

A communication link between each group of agents (subsection 5.2.2) and the network operator central system should still exist, in order to allow a certain degree of minimal monitoring and perhaps even control, in the case the decentralized system fails to maintain the necessary control of the network stability properties.

5.2.2 Agent Grouping

In a decentralized fashion scheme, it is not wise to expect all the agents of the network to communicate with each other as if they belonged to only one group, due to two factors: high loads of communicated data and geographical impediments. Therefore, it is important to gather agents in smaller geographically likely groups. Our suggestion for group formation is that, ideally, each agent belongs to a group of five agents. If we consider a very dense network such as the one shown in figure 5.2.1, then we can make each agent to communicate to other four agents. Each one of the other four agents has to communicate to the original agent and three others. This means that, with this ideal situation, a network disturbance, after 3 calculation steps has already reached 24 different nodes of the network.

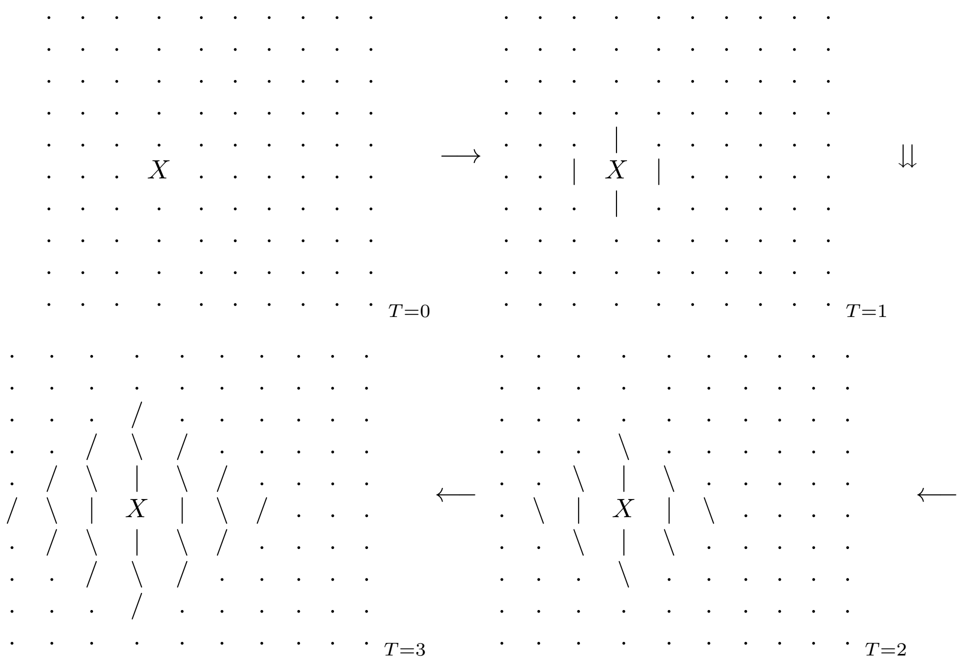

Figure 5.2.1 – Propagation of a perturbation from a single agent throughout the network
At $T = 0$ the node signalled with an "X" is subjected to a high ageing factor. In order to resolve that perturbation in the network stability, it communicates with its group. After the time step $T = 3$, 24 elements of the network were already notified about this perturbation and that mesh of agents can mitigate the issue.

In a real power grid, it is difficult to build a perfect matrix such as the one used for the example in figure 5.2.1. Given so, this type of grouping of agents should be looked at as a mere example of a possible solution. Upon implementation of such a system, the network operator has to take into account, not only the geographical distance between agents, but also what the electrical likeliness between them. With electrical likeliness, we mean that even if two agents are distance-wise very close by, they might be completely electrically decoupled and, if so, they can not interfere with each other health status. If that is the case, these two agents should not belong to the same group.

Disturbance propagation is important, as we enable the network to behave as a single organism built from decentralized small sub-sets of smart and autonomous agents, avoiding huge amounts of data communication and processing in a centralized point.

5.2.3 Synchronism

Each agent can be considered as a centralized point of action, as it has to gather all the data coming from all the other agents in its group of action. Given so, synchronism plays an essential role in the process. Within the time period between the last estimation/action step and the next one, all the necessary data from all agents need to reach all the other agents that belong to the same action group, in order to allow each agent to successfully compute an accurate state estimation and generate an optimal signal of action relative to the group it belongs.

This synchronism will be achieved by, such as in section 5.1.2, time-stamping all the data values expedited from each agent, not only to ensure that all datasets from the same time period reach its destination, but also to avoid datasets from other time periods to be evaluated in the current period.

Again, it is important to note that the time periods that we are dealing with here are significantly large to avoid synchronism issues. Nevertheless, it is something to take into account while building the specifications of the system. It must be clear, for example, that if an agent is geographically far from the other agents of its group, its datasets can sometimes, due to temporary low bandwidth availability (or some other latency factor), take too long to reach its target and perhaps miss the current time period calculation.

In the case that one agent fails to successfully propagate its dataset throughout all the other agents, the agents that did not have access to this missing link should still be able to compute the next step estimation. They should also be able to filter out the dataset, when it arrives after the current time period calculation has taken place. This estimation can be a bit biased due to the lack of full knowledge of the whole group state, but it will for sure better than if it did not take place at all.

5.2.4 Load Distribution Algorithm

The health state outputted by a single agent is not a representative value to achieve a grid stabilization until it is related to all the other agents outputs. Within one group of two agents, it can be the case that agent A predict its ageing factor to be 1.2 and agent B computes a value of 1.5. From the agent A perspective, if it did not have access to the agent B dataset, it seems that it should trigger a power rerouteing in order to lower its ageing factor of 1.2. If that would happen, then the power would probably be rerouted through agent B, which would cause even more deterioration of the group's ageing factor[5]. Given so, it is necessary for agent A to relativise its ageing factor with the group's ageing factor in order to properly evaluate what type of trigger should be fired. It is straightforward, in this case, that agent A will realize that its ageing factor should be increased in order to decrease the ageing factor of agent B and therefore lower the group's ageing factor.

When an agent computes its own health state and gathers all the datasets from the other agents in its group, it has full knowledge of the group's ageing factor and therefore can take the right action by relating his state to the group's. This is achieved through a simple averaging formula:

$$systemAgeingFactor_{predictionStep} = \frac{1}{n}\sum_{i=0}^{n} ageingFactor_{i,predictionStep} \tag{5.2.1}$$

Based on the system ageing factor and on its own ageing factor, each agent generates a signal that will trigger a certain action. On one hand, if its ageing factor is lower than the system's, then the agent creates a signal that triggers the action system in order to force more power to flow through it. On the other hand, in the case that the agent finds out that its ageing factor is higher than the system's ageing factor, then the signal it creates should trigger the action system to try to distribute the power that is planned to go through this agent among the neighbouring ones.

Averaging the system's ageing factor is a very simple but seemingly adequate solution for this problem. Even when the ageing factors of a group of 5 agents are 0.3, 0.4, 0.5, 0.6, and 0.7 it is wise to spend resources into bringing them into the average 0.5 ageing factor. Even though 0.7 is not a critical value to be concerned with, by having the 5 agents with a lower ageing factor value, there is a better margin of safety to solve possible future issues, whether they rise from inside the group or they come from external groups, as detailed in section 5.2.2.

[5] as we have shown before, the same amount of power increase is more detrimental for a power transformer with an higher ageing factor

5.2.5 Action System

The action system can be any available system capable of power rerouteing, as detailed in section 2.5. These action systems only need to react to the signals created by the agents in order to distribute the ageing factor as homogeneously as possible and, with that, make the best use of the available network resources.

In this chapter, we assume that all power transformers have controllable on-load tap changers and that, by making use of them, power can safely be rerouted to other branches of the network. Although we are aware that tap changers are used to regulate the voltage on the output of the transformer and that power rerouteing is, most of the times, achieved by the usage of phase shifters, we make use of the tap changers for two reasons:

1. It works, because if one increases the voltage on the secondary side and maintains the same voltage on the primary side (by increasing the turn ratio), in order to keep the system stability, the power flow simulation forces the power to flow through other branches;
2. As the action system is not the main focus of this work, we make use of the tap changers as they are, computationally, the easiest to integrate in the framework.

We assume also that the tap changers of the transformers have a default value of 1 and can be shifted up and down by at most 15%, being the minimum and maximum values 0.85 and 1.15, respectively. Also, the variation steps have to be discontinuous in time and they have a maximum value of 1%, so 0.01 in absolute value.

As the tap changer is an internal asset to the agent (as we assume the agent to be the electrical hardware plus the control systems), we let the actuator from figure 4.1.2, directly interpret the signal generated by the local planner and adapt the turns ratio of the transformer according to what is requested by the local planner. If the planner decides that more power should go through the transformer, due to foreseen damage on neighbouring transformers, then the actuator decreases the turn ratio of the transformer, so that the power will tend to go more through this transformer. If the planner's decision is to distribute power through the neighbours, then the actuator takes the opposite action and increases the tap changer by one step. On the next time period, another step in the tap changer is taken, making it vary every minute, unless it already reached the maximum or minimum value.

5.2.6 Computational Power

The computational power of each agent will be dependent, not only on the number of calculation layers present in its predictive health model as stated in section 5.1.3, but also on the size of the group where it belongs to, i.e. the number of other agents that will communicate with it. The larger the number of agents one agent has to communicate with, the larger the amount of data it has to handle and therefore the larger memory it has to have.

About the processing power, the only addition to the case discussed in section 5.1.3 is the calculation of the system's average ageing factor and a simple comparison achieved by the local planner. Given so, we can still consider this process to be a non computationally demanding action.

5.2.7 Practical Implementation and Results

Based on the implementation discussed in section 5.1.4, the only extra steps added in order to achieve the decentralized control are:

- Replace the communication between agents and the central action control point with communication between the three agents - that are, in this case, a single action group;
- Enable the agents to control the tap changers of their corresponding transformer;

The remaining simulation specifications are exactly the same as in section 5.1.4.

5.2.8 Simulation with Agents with Control

In this simulation, the exact same steps are taken, the initial variables are the same, and the power flow as well. The major difference in this case is that at every step in time the agents will talk to each other in order to exchange their predicted ageing with all the other agents. In this way, at every time step, each agent has access to all the agents predictions of ageing over the next 30 minutes. Based on all those values and equation 5.2.2, each agent is capable of locally computing a global average of the predicted ageing of the system within the prediction time frame following this equation:

$$sysAgeingFactor_{30mins} = \frac{1}{3}(aFactor_{56,30mins} + aFactor_{47,30mins} + aFactor_{49,30mins}) \quad (5.2.2)$$

After this computation, the agent has sufficient data about itself and the global system to be able to evaluate its own condition by relating it to the system's condition. This calculation takes place in the local planner (figure 4.1.2) and its outcome is a signal that enters directly in the actuator. The actuator is equipped with a system that, depending on the input signal, can increase or decrease the transformer ratio, by making use of the tap changers. In the IEEE 14 bus network specifications it is said that the transformers of this network have a fixed turns ratio. Nevertheless, in order to show the possible effect of this type of action in a network, we assume that these transformers have an adaptable ratio that can vary $\pm 15\%$ (from 0.85 up to 1.15) in steps of 1% (0.01). Basically, each agent compares its predicted ageing with the system's ageing and if the agent is over the average, then the transformer is being subject to a stress that perhaps could be split among the other transformers of the network that are pushing the average value down. In this case, the local actuator of this overstressed transformer takes

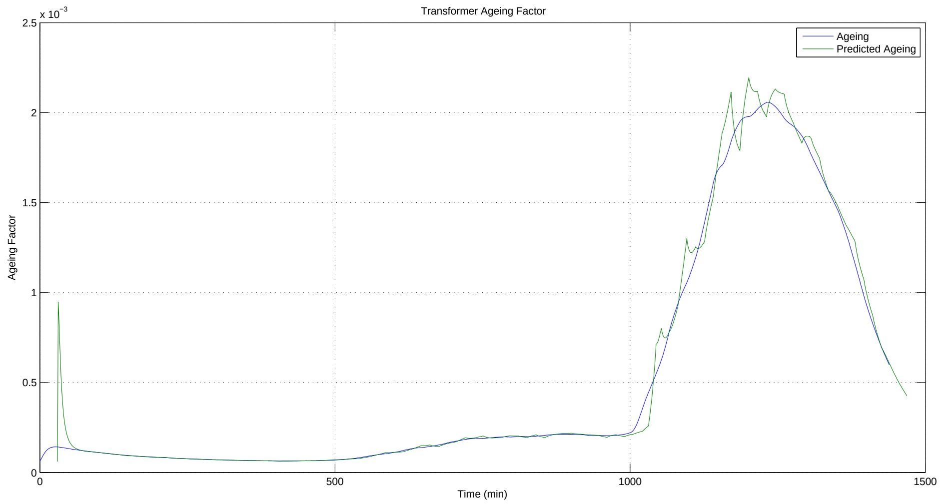

Figure 5.2.2 – Ageing Factors of Controlled Transformer 4 to 7
The blue curve is a computation of the controlled transformer ageing factor in real time and the green curve is a computation of a 30 minutes prediction. The initial peak in the green curve is a result of the steep increase of the hot-spot temperature shown in figure 4.2.2. The peak is so visible because the model assumes that the increase of the hot-spot temperature will be steady over 30 minutes.

action in the tap changer and increases the value of the transformer ratio. On the contrary, the agents that detect that their transformer will age less than the average can decrease the ratio of the transformers. The result of this combined action should make it easier for the power to flow through the less stressed transformers and therefore diminish or even avoid the detrimental results shown in the section 5.1.5. This control-action procedure from the agents only starts taking plane after minute 1000, as that is roughly the point where the most interesting load behaviour takes place.

By proceeding with these objectives, the new results follow can be found in figures 5.2.2, 5.2.3, and 5.2.4.

Given the results show in table 5.2, a large set of conclusions can be taken, but the most important ones are:

- the considerable reduction of the system's ageing from $0.23 + 0.02 + 457.53 = 457.78$ minutes to only $0.60 + 0.03 + 94.82 = 95.45$ minutes, which consists of a reduction of almost 80%. Such a large gain in the lifetime loss of the power assets is reached by a mere re-routeing of power flow in the right moment - i.e. early enough - from the branch 5 to 6 into the other two branches. It is remarkable to note that although the amount of power rerouted from branch 5-6 is only around $76pu(13\%)$, the reduction of lost lifetime is

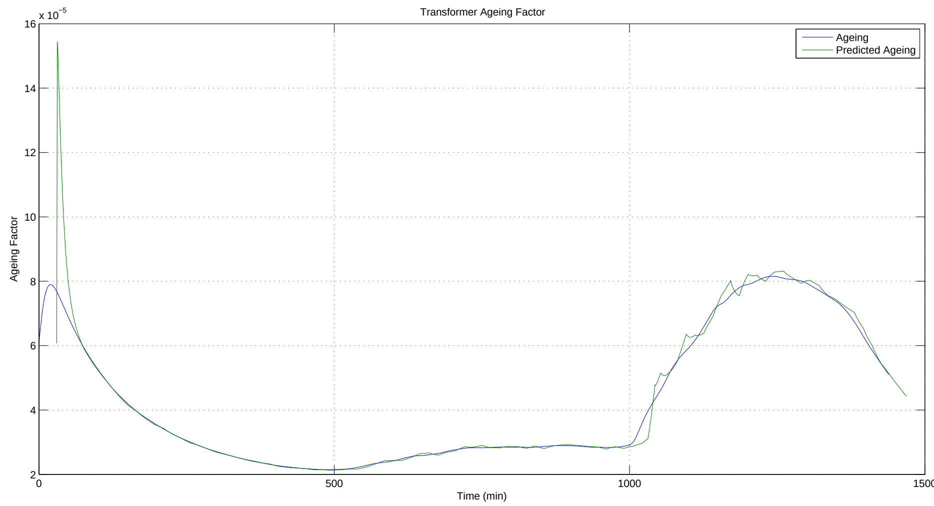

Figure 5.2.3 – Ageing Factors of Controlled Transformer 4 to 9
The blue curve is a computation of the controlled transformer ageing factor in real time and the green curve is a computation of a 30 minutes prediction. The initial peak in the green curve is a result of the steep increase of the hot-spot temperature shown in figure 4.2.2. The peak is so visible because the model assumes that the increase of the hot-spot temperature will be steady over 30 minutes.

Table 5.2 – Simulation Summary - Controlled

Transformer	Ageing (mins)	Pred.Ageing (mins)	Error (mins)	Error (%)	Power Flow (pu)
4-7	0.59537	0.62056	0.02519	4.23	315.4072
4-9	0.029152	0.029965	0.000813	2.79	182.1552
5-6	94.8229	97.7505	2.9276	3.09	509.3345

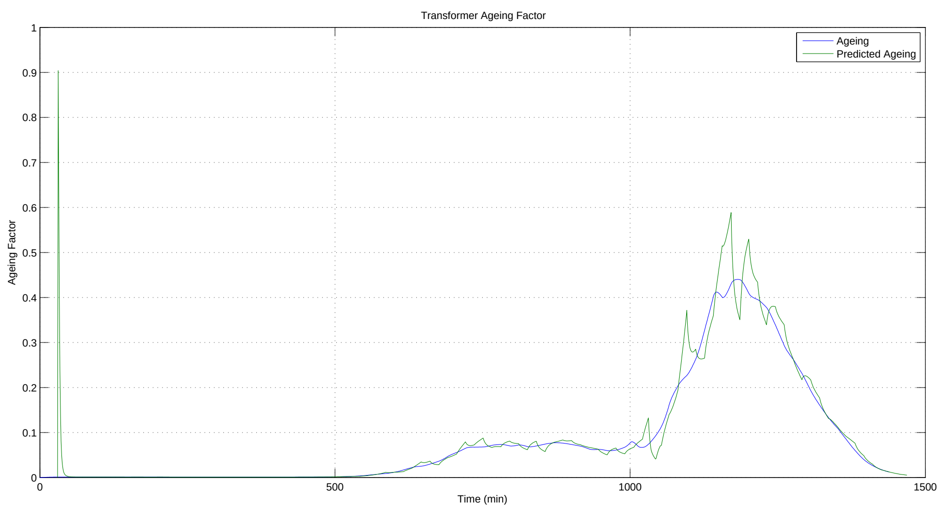

Figure 5.2.4 – Ageing Factors of Controlled Transformer 5 to 6
The blue curve is a computation of the controlled transformer ageing factor in real time and the green curve is a computation of a 30 minutes prediction. The initial peak in the green curve is a result of the steep increase of the hot-spot temperature shown in figure 4.2.2. The peak is so visible because the model assumes that the increase of the hot-spot temperature will be steady over 30 minutes.

around $362.7min(80\%)$. On the other hand, these $76pu$ of power that are now transmitted through branches 4-7 and 4-9 do not have almost any impact on the lifetime consumption of the corresponding power transformers, as they are operating far below their thermal limitations.

- the prediction errors are, in this case, even more accurate than with an uncontrolled system, as the average error is only 3.37%.
- the behaviour of the transformer ratios is relatively predictable in this case, as the situation only involves three transformers and only one is considered to be in a critical ageing situation. Given so, as the control action starts taking place (from the $1000th$ minute on), the tap changers are immediately triggered by the corresponding actuators in order to increase the transformer ratio of the transformer 5-6 up to 1.15 and decrease the other two transformers ratios to the minimum of 0.85. As stated before, this changes are accomplished by actuating on the tap changer with steps of one minute and therefore, the final statuses of 1.15 and 0.85 in the respective transformers are only completely reached after around 20 minutes of simulation (the starting point of the transformer ratios of this network is not uniform).

5.3 Immediate Cost Reduction

From sections 5.1 and 5.2, immediate cost reductions can be expected. If we do not regard the cost of equipping the electrical network with the extra hardware, and we only use the insulation ageing as a cost factor (as depicted in equation 2.3.4), then the cost reduction of having a controlled action system applied to the network active during $440mins$[6] can be calculated with the following method, by assuming that an insulation failure results in a total transformer failure:

Given the example that each transformer has a cost of $5M€$ and an estimated lifetime of 20 years, then the total cost of one minute of lifetime is around 0.475€[7]. In the example from section 5.1, the cost of the lost lifetime in the system's transformers is about 226€[8] whereas on the example from section 5.2, the cost of the lifetime loss is only 45€[9]. Looking at it in this way does not really cause a significant result as we are comparing a few tens of Euro with $5M€$. If we state that this small network is indeed a planning failure and that this phenomenon happens every day of the week, then it is reasonable to say that within five years the first example will generate a cost of 412450€[10] and the second example will achieve much better results, by

[6] as the control system was activated only after the $1000th$ minute

[7] $\frac{5000000}{(20\times 365\times 24\times 60)}$

[8] 0.475×475.78

[9] 0.475×95.45

[10] 226×1825

generating a cost of only 82125€[11]. Not only does this show an extremely high cost for the utility, but also it is important to note that if the transformer 5-6 has already aged 19.5 of the estimated 20 years of lifetime (still 262800 minutes available), then in the first example it will fail after 552 days. However, on the second example this transformer will still be able to operate for more 2753 days, which means more than 7.5 years.

5.4 Summary and Conclusions

Whether we talk about the centralized (section 5.1) or the decentralized (section 5.2) version of the agents introduction in the Electrical Power Grid, the benefits are unequivocal. In the centralized version of the system, although from the network operator view, the control scheme seems to be the same (as the operator still manages the network from an action-control centre), that is absolutely not the case. With the inclusion of agents in the grid components, the network operator has access to a set of factors of major importance, such as the current ageing factor of each component of the grid and a prediction of the same value within a variable prediction horizon. It is important to note again that this prediction horizon, that was in this chapter's simulations of thirty minutes, can be a different one, as further detailed in section 4.2.2.5. In the decentralized version of the system, the network operator can still expect a valuable monitoring resource provided by the links between each agent's group and the action-control centre. Nevertheless, most of the benefits inherent to the decentralized model regard the automated control action that occurs among the agents.

There are several factors that can be highlighted from this chapter:

- from the centralized scenario we take that a difference of 119% in transported power can lead to a difference of 200000% in ageing factor;
- the prediction of ageing factor seems to be quite an accurate method for the used step value - 30 minutes - as the error stands to be only 7% and 3.37% in the decentralized and centralized versions, respectively;
- the prediction ageing factor provides both the agents and the network operator a key asset to avoid unnecessary asset ageing, as for example at around the minute 1050 from figure 5.1.3, the predicted ageing factors were already around 1.7, while the actual ageing factor was still lower than 0.3;
- agents can effectively be gathered in groups of five units, in order to generate a node of the decentralized network - in the end, each agent can only communicate with four others;
- the automated system set-up in section 5.2 by itself was able to highly decrease the possible ageing of the three power transformers of the network by 362.7 minutes - 80% - just by

[11] 45×1825

rerouteing 76*pu* - 13% - of the total transmitted power;

- from section 5.3 we conclude that a day of simulation costs about 45€and 226€ for the uncontrolled and the controlled simulations, respectively;
- a power transformer with a remaining lifetime of half an year, will fail after 552 and 2753 days - 7.5 years - in the uncontrolled and controlled simulations, respectively.

Chapter 6

Discussion

6.1 Effect of Temperature Cycling and HF Transients

In the context of further investigating the results presented on the existing literature, the author repeated a set of laboratory experiments in which oil-impregnated paper samples are subjected to different values of temperature and high frequency transients. The results of the experiments are acquired by performing a $\tan\delta$ assessment on the material.

After performing tests with non-stresses samples, samples stressed with AC only at $40^{\text{o}}C$, and samples stressed with AC + $5kHz$ transients also at $40^{\text{o}}C$, the results suggested that an introduction of $5kHz$ transients in the line voltage could improve the dielectric properties of oil-impregnated paper insulation. Given the fact that this result is counter-intuitive and also goes against the results of [9] that the author was trying to reproduce, this verification attempt has been dropped.

Several reasons can be identified for the considerable discrepancy of results, such as:

- a different laboratory operator;
- deterioration of the used materials;
- small amount of results;
- high sensitivity of the measured entities (10^{-4});
- possible presence of moisture or impurities in samples, as their existence is also dependent on the way the samples are handled.

6.2 Framework of Model-Based Optimization

The proposed framework of model-based optimization resulted in explicitly successful results. By allowing power network components, such as a power transformer, to be automatically monitored and controlled by a single agent that implements the aforementioned framework, it has been show that we can improve the utilization of the available resources.

In chapter 4, we have seen that, by limiting the ageing factor of a power transformer to unity, and plugging the transformer's thermal models detailed in section 2.2 into the framework, the agent has automatically and autonomously solved the over-ageing issue by rerouteing power to other available network components. Simple simulations of one regular day in operation have shown that it is possible to spare a power transformer's available lifetime by more than 40%, just by rerouteing 0.78% of the total power transported by the transformer throughout the day. This large difference between the cost and the profit must be emphasized. From these simulations it results that it can be very profitable to reroute the right amount of power at the right time if we talk about power network component's lifetime. The key point here is that this type of system, not only shows us that it can be profitable to do it at the right time, but also provides the network operator, or any other type of actuator, with the necessary data to know when to do it.

As previously mentioned, for the actuator, it is as important that it has to perform a preventive action as it is when the action is supposed to be performed. To enable the actuator to create better results, its actions have to be based on accurate data. The agent's output set encompasses a health state estimation of the next time step in the simulation. Given the fact that the simulation step can be modified, a comparison between different time steps has also been performed. The results show that when the agent's time step is increased, intuitively, the estimation's accuracy decreases and more power has to be rerouted. This is the price to pay if the power network operator needs to reduce computational and/or communication network usage.

Overall, it has been shown that for time steps lower than 60 minutes, the rerouted power for the same example simulation (so for the same 40% decrease in the power transformer's ageing) is lower than 5.27%. If we compare the increase of rerouted power between the time steps of 1 and 60 minutes to the decrease in computational and network consumption, it is straightforward that the gain in computational power is 60 times and the increase in rerouted power is just around 5 times. Of course, it is then up to the network operator to decide whether 60 times of decrease of computational power are more or less relevant than the increase of 5 times the rerouted power. It is important to note that thiese kinds of decisions are all up to the network operator, as they can highly vary based on, for example, the local network topology. If the neighbouring network provides several options for power rerouteing, then the network can locally value the computational power rather than the power rerouteing rate.

About the inclusion of high frequency transients in the simulation waveform, the incremental factor of 6.4%, that refers to the aforementioned "transient mix" value, over the accelerated ageing factor causes the controlled system to start rerouteing power 1 minute earlier and it only stops rerouteing power 4 minutes after when compared to the example with a live voltage clear of high frequency transients. In this case we can also see that the component's lost lifetime is about 2.27% and 6.4% higher in the controlled and uncontrolled simulations, respectively, while comparing the high frequency scenario to the previous one. In the controlled case, the increase of the lost lifetime is not so considerable as in the uncontrolled scenario. This is the case, because the accelerated ageing factor variation with the hot-spot temperature is not a linear relation, as it increases faster for higher temperatures. This means that in the uncontrolled simulation, the "transient mix" causes more damage than in the controlled scenario.

All in all, it is important to note that, not only the results are interestingly favourable, but also the proposed framework shows to be easily scalable in terms of the number of utilized modelling layers on top of the electrical component.

6.3 Introduction of Agents in the Electrical Power Grid

The introduction of agents in the electrical power grid, has been shown to be beneficial on both discussed topologies - centralized and decentralized. Given the criticality of some aforementioned results, such as the reduction of 40% of lost lifetime of a component with a mere reduction of 0.78% of the transmitted power, it turns out fundamental to include monitoring tools in the in place over-aged electrical power grid.

In the centralized scenario, we have seen that the overall grid topology does not have to be modified, apart from the addition of communication links between the all agents and the action control centre. In the decentralized scenario, the number of communication links between the agents and the monitoring/control centre is dramatically reduced by the fact that only one agent from each group communicates the group's status back to the monitoring/control centre. Between agents of the same group, the topology is much more complicated in the decentralized scenario, for a complete communication network has to be built in order to enable the agents to exchange relevant data that will allow them to compute decisions.

Although monitoring by itself is already extremely useful, the fact that agents can take part in the control actions generates some surprisingly interesting results. In the presented example, the automated system set-up by itself was able to highly decrease the possible ageing of the three power transformers of the network by 362.7 minutes - 80% - just by rerouteing $76pu$ - 13% - of the total transmitted power of the full day of operation. In contrast with chapter 4, in the current case, the rerouted power ends up being rerouted by the existing power transformers in the network. As so, it is important to mention that the amount power delivered to the consumer is the same with or without the agents control.

The utilized prediction horizon of 30 minutes results in a considerably accurate reference value, as the error stands to be only 7% and 3.37% in the decentralized and centralized versions, respectively. The network operator can increase this value, if the objective is to enhance the predictability of the system, although it will result in larger errors. Another option is to increase the number of outputs each agent can exchange among each other and make use of another type of algorithm that looks at, for example, the current value, and both values of 30 and 60 minutes. This type of algorithm would ideally try to create a balance between predictability and the error.

In the shown examples, as the electrical power grid only contained three power transformers, we opted to enable communication between all agents. Nevertheless, in more complex cases, it is recommended to decrease the communication complexity by the creation of smaller groups of agents. Given so, each agent only communicates with the other agents in its own group. There is also a main agent in each group that communicates back to the monitoring centre. The proposed number of agents per group and the type of communication strategy proposed in this document is highly generalized. For we assume the existence of a very dense matrix-like network in which the network operator can always create groups of 5 agents. This is, of course, not the case in real electrical networks, as the position of power transformers in the network will respect geography rather than geometry. With this, we mean that if the geographical status of the power transformers does not allow grouping and communication as suggested, then the network operator has the flexibility to adapt the rules, in order to produce a better strategic result. All in all, each network will need some kind of customization, for it is difficult to project a globally working solution.

The overall result of the decentralized simulation with control on the agents side is rather inspiring. The presented simulations show a very good example of its benefits, as by the minute 1050 from figure 5.1.3, the predicted ageing factors were already around 1.7, while the actual ageing factor was still lower than 0.3. This result is a key starting point towards the implementation of agents in the current power grid, as it unmistakably shows the value of decentralized monitoring and control through the actions of automated agents. Nevertheless, there are also some issues with this type of monitoring-control systems, as one can see, for example, with the initial peak that occurs in figure 5.2.4 that is a result of the initial quick increase in the hot-spot temperature shown in figure 4.2.2 at around the same instant. This high peak occurs, because the 30 minute estimation assumes that the system will behave over the next 30 minutes exactly the way it has behaved during the last minute. Rapid increases of the hot-spot temperature can therefore generate such undesirable peaks that will probably trigger the agent into taking actions to reroute power, although in this example it did not have to. This problem could be addressed by including a safety margin to the algorithm, in which the agent would not react until the data shows to be consistent over a certain minimal period of time. We reach again a balancing challenge, as the network operator will have to posit what the ideal situation is, between false alarms and real dangerous situations. As with all other systems, if one puts the false alarm boundary too high, it can generate overlooked important situations. Moreover, another type of error can occur by using such monitoring-control systems. If, at a certain moment in time, the hot-spot temperature decreases for a while and then starts dangerously increasing again, the system will interpret the initial decrease and propagate the information that the ageing factor will decrease over the next thirty minutes. As this is not the case, we can incur in an unnecessary overloading of a power transformer, because the system allows more power flow through it than it should. As the system is highly dynamic, the agent in cause will quickly acknowledge the error and revert the action requests, re-establishing the ageing stability of the power network.

A key factor that has been omitted in the specifications of the framework and its implementation is the inherent available lifetime of the components where the agents were built. Only the dynamic (under operation) ageing has been subjected to discussion. Nevertheless, it is straightforward that, for example, a power transformer with 1 year of available lifetime should be more watchful than a power transformer with 20 years of available lifetime. In this context, the available lifetime of a component in general should be part of the agent's calculation parameters, so that the system is able to provide more care to the most aged components.

In order to make the result more palpable, a translation between power transformer life-minutes and money is also suggested by the document. Following the earlier stated assumption that an insulation failure leads to a total component failure, it can be posited that each minute of lifetime costs a certain amount of money, as explained in section 2.3. Given so and, once again, referring to the example studied in section 5.2, it can be stated that a scenario that would cost 226€ over one operating day, can be reduced to just 45€, through the usage of the decentralized control system. This cost is only referent to the power transformer spent lifetime. These values will be different for different networks and load profiles. Nevertheless, with a correct implementation of the system (avoiding the possible flaws detailed in the previous paragraph), it turns out to be very difficult to produce worse results than with the absence of agents in the electrical power grid.

Chapter 7

Conclusion

7.1 Conclusions

7.1.1 Effect of Temperature Cycling and HF Transients

Following the line of thought sketched in section 6.1, the author opted to adopt some of the conclusions presented in [9]:

- The $\tan\delta$ decreases in the interval $40^{o}C$ to $80^{o}C$ when a sample is stressed with transients;
- The introduction of transients in the line voltage causes an average increase in $\tan\delta$ of 6.4%.

These results are valuable, as they allow us to further investigate about the health status of a given power network component, if oil-impregnated paper is used as its insulation system and there are high frequency transients present in the line voltage.

7.1.2 Framework of Model-Based Optimization

The posited framework of model-based optimization has proven to be a valuable asset at the single electrical power component level. By enabling a smart local planner to generate decisions based on data-sets coming from sensors and interpreted by physical models, several critical factors have been effectively optimised. The most important influenced factors are:

- a reduction of the lifetime loss during the power transformer's operation - e.g. a lifetime loss reduction by more than 40%, by rerouteing only 0.78% of the total power through the transformer;
- the estimation frequency can be varied in order to vary the need of computational and networking power. For a larger time step, less computational and networking power is

needed, but more electrical power ends up being rerouted due to the decrease of the agent's accuracy - time steps of 15 and 60 minutes, result in rerouteing 1.13% and 5.27% of power, respectively;

- the presence of high frequency transients is detrimental for the electrical components - the incremental factor of 6.4% over the FAA causes the controlled system to start rerouteing power 1 minute earlier and it only stops rerouteing power 4 minutes after the example with no high frequency transients;
- the increase of the LLT, in the presence of high frequency transients, is larger in the uncontrolled scenario, while compared to the controlled one. This is due to the fact that the FAA variation with the hot-spot temperature is not a linear relation, as it increases faster for larger temperatures. This means that in the uncontrolled simulation, the "transient mix" causes more damage than in the controlled scenario. The lost lifetime in the presence of high frequency transients is about 2.27% and 6.4% higher in the controlled and uncontrolled simulations, respectively, while comparing the high frequency scenario to the previous one.

7.1.3 Introduction of Agents in the Electrical Power Grid

Introducing agents in strategical nodes of the electrical power network has shown to be surprisingly beneficial for an efficient resource management. A communication network enables the agents to relate to the surrounding agents in order to distribute power components ageing in a uniform way throughout the entire electrical power network. This levelling up of power components ageing contributes to a better usage of the available power network resources. The most critical conclusions of chapter 5 are:

- it has been shown that for an increase of 119% in transported power through a transformer can lead to a difference of 200000% in its ageing factor;
- it is fairly easy to find an example where we see the agents improving the overall system's health status - the automated system set-up in section 5.2 by itself was able to highly decrease the possible ageing of the three power transformers of the network by 362.7 minutes - 80% - just by rerouteing $76pu$ - 13% - of the total transmitted power;
- the prediction horizon used in the simulations, 30 minutes, can be increased in exchange of prediction accuracy;
- the prediction ageing factor provides both the agents and the network operator a key asset to avoid unnecessary asset ageing;
- agents can effectively be gathered in groups of five units, in order to generate a node of the decentralized network;

- a power transformer's lifetime, which is a valuable asset, can be dramatically extended with the usage of the right tools.

7.2 Future Work Recommendations

This project has achieved an implementation of the suggested framework of model-based optimization that allows us to understand the numerous possibilities that can be produced with such kind of systems. In this section, the author suggests some possible routes to follow-up the reported work.

7.2.1 Effect of Temperature Cycling and Transients

- The stressing and measurement places should be as close as possible to avoid moisturization and contamination of the samples while transporting;
- The amount of time the sample is in the air to drain the excess of oil should be the same for all samples, so that not only the amount of moisturization and contamination, but also the quantity of oil present in the sample are the same;
- The measurement set-up could be built with a glass cover that allows a continuously filtering of moisture out of the oil, through the usage of vacuum suction.

7.2.2 Integration of Agents in the Electrical Power Grid

- Add more rules to the framework, so that transient variations of the hot-spot temperature are not assumed as meaningful data to trigger actions;
- Integrate the system in a a small-scale electrical network, in order to test the viability of things like:
    - agent grouping;
    - agent/central synchronism;
    - system security;
- Postulate about other methods of power rerouteing;
- Study the electrical stability of this smart grid;
- Further investigate the ideal parameters for specific network topologies;
- Include the current available lifetime of each power component as a key factor in the health status computation;
- Extend the framework on the power transformer level by adding more transformer models, for example, regarding asset robustness;

- Extend the framework's applicability by using it in other types of electrical components, such as cables, by replacing the used models with others that refer to cables.

7.2.3 Continue my work

The code that generated all the results of this project is publicly available at `https://github.com/grizonic/model_based_optimization_power_network`. Feel free to clone (`https://www.kernel.org/pub/software/scm/git/docs/git-clone.html`) the repository and use its contents for further development.

Bibliography

[1] - Energy Roadmap 2050 - Technical and Economic Analysis, European Union, Brussels, 2009

[2] - Analysis of Transformer Failures by William H. Bartley P.E., The Hartford Steam Boiler Inspection & Insurance Co.

[3] - Exploring the Feasibility of an Aging Model for Paper Insulation Based on the Repetition Frequency of Transients, T.L. Koltunowicz, G. Bajracharya, D. Djairam and J.J. Smit, Delft University of Technology

[4] - IEEE Guide for Loading Mineral-Oil-Immersed Transformers, 1995

[5] - IEEE Guide for Loading Mineral-Oil-Immersed Transformers - Corrigendum 1, 2002

[6] - Sustainable energy development - performance and prospects, Michael Jefferson, 2005

[7] - D. Susa, M. Lehtonen, and H. Nordman, “Dynamic thermal modelling of power transformers,” IEEE Transactions on Power Delivery, vol. 20, no. 1, pp. 197–204, January 2005.

[8] - L. W. Pierce, “An investigation of the thermal performance of an oil filled transformer winding,” IEEE Trans. Power Del., vol. 7, no. 3, pp. 1347–1358, Jul. 1992.

[9] - The Effect of Temperature Cycling and Transients on the Dielectric Properties of Transformer Impregnated Insulation, Bart Kers, 2011

[10] - Haefely. Haefely.com. [Online]. http://www.haefely.com/pdf/LL_2840_0410_LWA.pdf

[11] - E. Gulski, J.J. Smit, and J.P. van Bolhuis, "Monitoring and diagnostic of transformer solid insulation," IEEE, p. Vol.7 No.2, 2002.

[12] - R. D. Zimmerman, C. E. Murillo-Sánchez, and R. J. Thomas, "MATPOWER: Steady-State Operations, Planning and Analysis Tools for Power Systems Research and Education," Power Systems, IEEE Transactions on, vol. 26, no. 1, pp. 12-19, Feb. 2011

[13] - Lundgaard, L.E.; Hansen, W.; Linhjell, D.; Painter, T.J.; , "Aging of oil-impregnated paper in power transformers," Power Delivery, IEEE Transactions on , vol.19, no.1, pp. 230- 239, Jan. 2004.

[14] - J. Fabre and A. Pichon, “Deteriorating processes and products of paper in oil. Application to transformers,” in CIGRÉ, Paris, France, 1960, Paper 137.

[15] - B. Bouvier, “Noveaux critéres pour caractériser la degradation ther- mique d’une isolation à base de papier,” Rev. Gén. l’Elect., vol. 79, no. 6, pp. 489–496, 1970.

[16] - Renewable Energy into the Mainstream, IEA, Renewable Energy Working Party, 2002

[17] - Towards a Smarter Grid, ABB´s vision for the power system of the future, ABB Inc. report, USA 2009.

[18] - The smart grid – an introduction, (US) Department of Energy, 2008 [http://www.oe.energy.gov/SmartGridIntroduction.htm].

[19] - SmartGrids, European technology platform for the electricity networks of the future [http://www.smartgrids.eu/].

[21] - Hutchingson, Alex. "The New Energy Fixes: 10 Fixes." Popular Mechanics. June 2011: 73. Print.

[22] - Rowland, S.M.; Bahadoorsingh, S.; , "A Framework Linking Insulation Ageing and Power Network Asset Management," Electrical Insulation, 2008. ISEI 2008. Conference Record of the 2008 IEEE International Symposium on , vol., no., pp.732-736, 9-12 June 2008.

[23] - http://www.electricenergyonline.com/?page=show_article&mag=41&article=311, last accessed in June 2012

[24] - Guo, H.; Rudion, K.; Abildgaard, H.; Komarnicki, P.; Styczynski, Z. A.; , "Parameter estimation of dynamic load model using field measurement data performed by OLTC operation," Power and Energy Society General Meeting, 2012 IEEE , vol., no., pp.1-7, 22-26 July 2012

[25] - Giselbrecht, D.; Leibfried, T.; , "Modelling of Oil-Paper Insulation Layers in the Frequency Domain with Cole-Cole-Functions," Solid Dielectrics, 2007. ICSD ’07. IEEE International Conference on , vol., no., pp.59-62, 8-13 July 2007

[26] - Patsch, R.; Menzel, J.; , "Ageing and degradation of power transformers — how to interpret Return Voltage Measurements," Electrical Insulating Materials, 2008. (ISEIM 2008). International Symposium on , vol., no., pp.179-182, 7-11 Sept. 2008

[27] - Menzel, J.; Patsch, R.; Kamenka, D.; , "Measurement of the dielectric properties of paper-oil cables and the cellulose-oil insulation system of power transformers," Properties and Applications of Dielectric Materials, 2009. ICPADM 2009. IEEE 9th International Conference on the , vol., no., pp.1020-1025, 19-23 July 2009

[28] Baird, P.J.; Herman, H.; Stevens, G.C.; , "Rapid Non-Destructive Condition Assessment of Insulating Materials," Electrical Insulation, 2008. ISEI 2008. Conference Record of the 2008 IEEE International Symposium on , vol., no., pp.742-745, 9-12 June 2008

[29] - Qian, Z.; Yan, Z.; , "Fuzzy synthetic method for life assessment of power transformer," Science, Measurement and Technology, IEE Proceedings - , vol.151, no.3, pp. 175- 180, 2 May 2004

[30] - Yan, Z.; Dong, M.; Shang, Y.; Muhr, M.; , "Ageing diagnosis and life estimation of paper insulation for operating power transformer," Solid Dielectrics, 2004. ICSD 2004. Proceedings of the 2004 IEEE International Conference on , vol.2, no., pp. 715- 718 Vol.2, 5-9 July 2004

[31] - Schafer, M.; Feser, K.; , "Thermal monitoring of large power transformers," Electric Power Engineering, 1999. PowerTech Budapest 99. International Conference on , vol., no., pp.98, 1999

[32] - Mirzaie, M.; Gholami, A.; Tayyebi, H.; , "Thermal Degradation of Cellulose Paper Insulation in Power Transformers," Solid Dielectrics, 2007. ICSD '07. IEEE International Conference on , vol., no., pp.673-676, 8-13 July 2007

[33] - Martin J. Heathcote, The J&P transformer book. Oxford UK: Elsevier Ltd., 1999 (12th edition).

[34] - Grilo, A.; Casaca, A.; Pereira, P.; Buttyan, L.; Goncalves, J.; Fortunato, C.; , "A Wireless Sensor and Actuator Network for improving the electrical power grid dependability," Next Generation Internet (NGI), 2012 8th EURO-NGI Conference on , vol., no., pp.71-78, 25-27 June 2012